Breaching-related turbidites in fluvial and estuarine channels

Examples from outcrop and core and implications to reservoir models

van den Berg, J. H.; Martinius, A. W.; Houthuys, R.

DOI
10.1016/j.marpetgeo.2017.02.005

Publication date
2017

Document Version
Final published version

Published in
Marine and Petroleum Geology

Citation (APA)
van den Berg, J. H., Martinius, A. W., & Houthuys, R. (2017). Breaching-related turbidites in fluvial and estuarine channels: Examples from outcrop and core and implications to reservoir models. *Marine and Petroleum Geology*, *82*, 178-205. https://doi.org/10.1016/j.marpetgeo.2017.02.005

Marine and Petroleum Geology 82 (2017) 178–205

Contents lists available at ScienceDirect

Marine and Petroleum Geology

journal homepage: www.elsevier.com/locate/marpetgeo

Research paper

Breaching-related turbidites in fluvial and estuarine channels: Examples from outcrop and core and implications to reservoir models

J.H. van den Berg [a, *], A.W. Martinius [b, c], R. Houthuys [d]

[a] Utrecht University, Faculty of Earth Sciences, Utrecht, The Netherlands
[b] Statoil ASA, Statoil Research Centre, Trondheim, Norway
[c] Delft University of Technology, Delft, The Netherlands
[d] Independent Consultant, Halle, Belgium

ARTICLE INFO

Article history:
Received 14 September 2016
Received in revised form
31 January 2017
Accepted 4 February 2017
Available online 6 February 2017

Keywords:
Breaching
Subaqueous slope failure
Turbidite
Massive sand
Spaced planar lamination
Reservoir properties

ABSTRACT

An understanding of the paleoenvironment and the main sedimentary processes behind preserved deposits is crucial to correctly interpret and represent lithofacies and facies associations in geomodels that are used in the hydrocarbon industry, particularly when a limited dataset of cores is available. In this paper a fairly common facies association is discussed containing massive sands - here defined as thick (>0.5 m) structureless sand beds devoid of primary sedimentary structures, or with some faint lamination - deposited by mass failures of channel banks in deep fluvial and estuarine channels. Amongst geologists it is generally accepted that liquefaction is the main trigger of large bank failures in sandy subaqueous slopes. However, evidence is mounting that for sand deposits a slow, retrogressive failure mechanism of a steep subaqueous slope, known as breaching, is the dominant process. A model of breaching-induced turbidity current erosion and sedimentation is presented that explains the presence of sheet-like massive sands and channel-like massive sands and the sedimentary structures of the related deposits. Sheet-like packages of spaced planar lamination that are found together with massive sand bodies in deposits of these environments are identified as proximal depositional elements of breach failure events. The model, acquired from sedimentary structures in deposits in the Eocene estuarine Vlierzele Sands, Belgium, is applied to outcrops of the Dinantian fluvial Fell Sandstone, England, and cores of the Tilje and Nansen fms (Lower Jurassic, Norwegian Continental Shelf). The possible breach failure origin of some other massive sands described in literature from various ancient shallow water environments is discussed. Breach failure generated massive sands possibly also form in deep marine settings. The potentially thick and homogeneous, well-sorted sand deposits bear good properties for hydrocarbon flow when found in such an environment. However, in case of deposition in an estuarine or fluvial channel, these sand bodies are spatially constricted and careful facies interpretation is key to identifying this. When constructing a static reservoir model, this needs to be considered both for in-place volume calculations as well as drainage strategies.

1. Introduction

One of the main challenges of lithofacies analysis of sedimentary successions in outcrop and particularly in the subsurface (using core) is to understand depositional processes and apply that understanding to interpret the local depositional sub-environment with the lowest degree of (preferably quantified) uncertainty possible. Depositional processes that formed individual lithofacies are considered in association with surrounding and genetically related lithofacies to reconstruct the sub-regional depositional environment. In the hydrocarbon industry, this qualitative understanding is used to build accurate three-dimensional geomodel representations of facies associations and the stratigraphic architecture. To achieve this, quantified data on geometries, external dimensions and internal heterogeneities is required. These static geomodels are normally built at specific scales of heterogeneity assumed to represent lithofacies (for example, a cross-stratified bed) and/or facies association objects (for example, a tidal bar). In order to represent all relevant heterogeneities of a hydrocarbon

* Corresponding author.
E-mail address: j.h.vandenberg@uu.nl (J.H. van den Berg).

http://dx.doi.org/10.1016/j.marpetgeo.2017.02.005
0264-8172/

reservoir, static geomodels are integrated and used in an upscaling methodology to result in a reservoir-scale geomodel that accurately represents the effects of rock properties on hydrocarbon flow at all heterogeneity scales (Nordahl and Ringrose, 2008; Ringrose et al., 2008; Keogh et al., 2014; Nordahl et al., 2014). Multiscale geomodels are crucial to understand possible fluid flow pathways at specific heterogeneity levels, evaluate drainage strategies, and estimate how much hydrocarbon is producible initially and progressively during the lifetime of a field.

Consequently, it is important to correctly interpret and represent lithofacies and facies associations in geomodels. This is the more challenging when a limited dataset is available. Offshore hydrocarbon fields typically have a minute core database available compared to the total volume of rock in the reservoir. A data set on the possible range of geometries, external dimensions and internal heterogeneity structure as well as the porosity and permeability structure of facies associations is therefore key input to any geomodel. For a valid assumption of these ranges, a correct interpretation of the main depositional processes and environments involved is crucial.

In this paper, we focus on a thus far hardly recognized but probably fairly common facies association formed by breaching and associated deposition of turbidites in deep fluvial and estuarine channels. We present new, additional results to the analysis of depositional processes of breach failure related deposits in the Vlierzele Sands, Eocene, Belgium, presented by Van den Berg et al. (2002), in order to support the recognition of similar deposits elsewhere. These deposits appear as homogeneous and to a large degree structureless sandstones and have limited lateral dimensions but can reach significant thicknesses (of more than 10 m). They can easily be misinterpreted in core if key criteria are not captured, which may lead to erroneous estimations of dimensional properties.

After stressing the importance of breaching as a failure mechanism in sandy slopes a depositional model of breach failure related deposits is presented. Subsequently, we apply this model to a well-known case in outcrop of fluvial deposits of the Fell sandstone (Dinantian, N. England) and core of the Tilje and Nansen fms (Lower Jurassic, Norwegian Continental Shelf) and discuss implications for geomodelling. In addition, the possible breach failure origin of massive sand deposits in some other environments is discussed.

2. Large slope failures in sand: liquefaction vs. breaching

In large slope failures in fine sand, such as frequently observed in banks of estuarine channels in the SW Netherlands (Fig. 1), mainly two contrasting processes operate, *breaching* and *liquefaction*. Liquefaction involves the sudden undrained collapse of the sand fabric, leading to an increase of pore water pressure that results in a dramatic reduction of shear strength and consequently instability of the slope. While liquefaction may occur in loosely packed contractant sand (with porosity > 43%), breaching is common in densely packed dilatant sands (Van den Berg et al., 2002). Liquefied channel bank failures typically result in debris flows, that deposit sediment *en masse*. Sand is called dilatant when, subject to shear deformation, its volume expands, causing a negative pore pressure with respect to the hydrostatic. The underpressured pore water "glues" the sand grains together and is able to maintain a steep (up to vertical) subaqueous slope. This slope only fails gradually, because the negative pore pressure is released slowly by water flowing in from the ambient fluid (Van Rhee and Bezuijen, 1998; Van den Berg et al., 2002). During the grain-by-grain failure the negative excess pore pressure dissipates locally, which weakens the deposit near the interface with the water, ultimately resulting in a thin surficial slide (Meijer and Van Os, 1976; Van Rhee and Bezuijen, 1998). This thin skin slide causes unloading and a drop in pore pressure, which strengthens the deposit and switches the slope failure process back to the grain by grain mode. The cyclic switch of failure process was named "dual-mode dilative failure" by You et al., 2014. However, as the grain by grain and thin skin failure processes are inextricably linked to each other, they are an intrinsic property of breaching. Therefore, the proposed new term is not justified and also misleading, because it erroneously suggests another type of failure.

While a flow slide failure in sand produces a debris flow, breaching initiates a well-defined turbidity current at the steep face of the retrograding breach. This provides a basis for distinguishing between deposits from the two types of flow, as long as debris flows are not diluted into a turbidity current. Because of the limited slope length in tidal and fluvial channels the distinction between a liquefaction and a breaching origin can possibly be made for most deposits that originated in proximity of a large subaqueous slope failure in fine sand in these environments. Unconfined breaching-related turbidites, which are thought to occur relatively frequently in margins of coastal and deeper waters, will remain more challenging to identify.

The main difference between a deposit of a turbidity current and a debris flow is that a turbidite is laid down incrementally layer by layer, whereas a sandy debrite is deposited in an *en masse* fashion (e.g. Talling et al., 2012). The latter process results in a diamict without primary sedimentary structures or at most some contorted bedding. In contrast, a turbidite generally shows some variant of the 5-partite Bouma succession of sedimentary structures (Bouma, 1962).

Thick divisions of homogeneous, largely unstratified sands are a common and often volumetrically important component of ancient deep-water turbidite successions (e.g. Kneller and Branney, 1995; Stow and Johansson, 2000). Although much less common, massive sands are also described from a number of ancient fluvial and estuarine channel deposits. They are often interpreted as sandy debrites originating from flow slide failures (Jones and Rust, 1983; Monro, 1986; Rust and Jones, 1987; Turner and Monro, 1987; Martin, 1995; Hjellbakk, 1997; Martin and Turner, 1998). One case of such type of massive sands in ancient deposits has been reported from an estuarine setting (Van den Berg et al., 2002). In this case, however, it was concluded that the massive sands are related to breach failures or at least failures dominated by breaching. Indeed, the presence of faint lamination proved that the deposition must have occurred incrementally layer by layer.

Breaching was first identified and studied in the 1970s by the Dutch dredging industry. The mechanism remained unknown to the geological society for decades, partly because the research effort in the Netherlands was largely performed in secret for proprietary reasons. A second reason is that breach failure events are easily mistaken for the well-known liquefied slope failure, because both failures produce a similar after-event morphology and are triggered in fine sand under similar environmental conditions (Van den Berg et al., 2002). Only recently it became clear that breaching may be an important source of turbidity currents in subaqueous canyons or any other subaqueous setting where sufficient fine sand can accumulate. Although direct observations of breaching events are rare and restricted to tidal channels (Van den Berg et al., 2002; Mastbergen et al., 2016) and tidal inlets (Beinssen et al., 2014; Beinssen and Neil, 2015), indirect evidence is mounting that large slope failures in sand are dominated by breaching:

- The presence in multibeam sounding images of series of upstream-migrating steplike bedforms, known as cyclic steps (Parker, 1996), that start directly downslope of submarine failure scarps (Smith et al., 2007; Paull et al., 2013; Casalbore et al.,

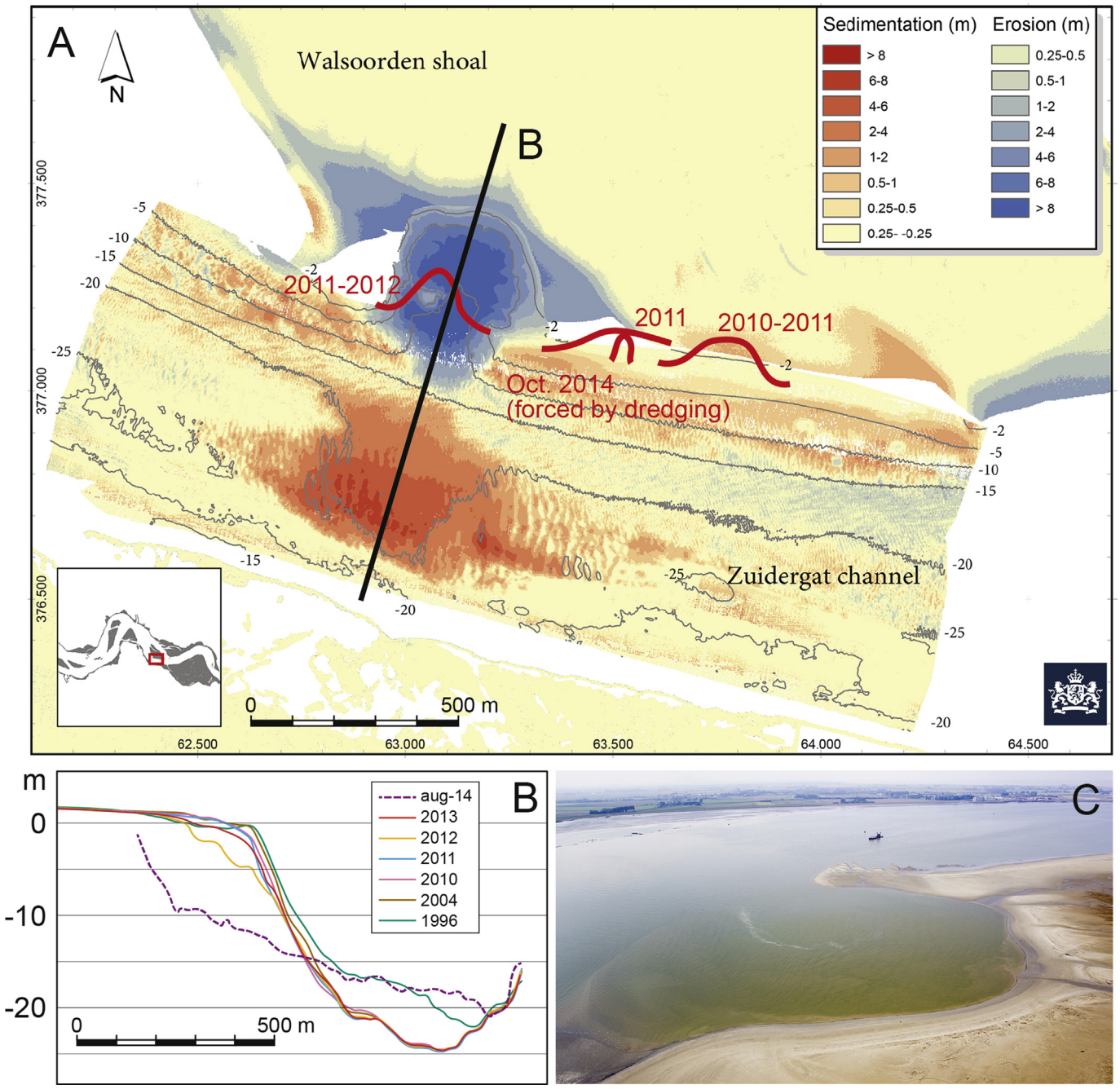

Fig. 1. A bank failure in the eastern part of the Western Scheldt estuary, 22 July 2014 comprising a volume of 0,8 million cubic meters A. Sedimentation – erosion patterns based on pre- and post-event multibeam soundings (Zuidergat channel: 8 July 2014 and 29 July 2014; post-event crater: 28 April/7 May 2014 and 21 August 2014; Walsoorden shoal: laser altimetry March 2014 and March 2015). Also indicated are scars of other recent bank failures over the past few years recorded on the shoal and the location of the bank failure experiment, October 2014; B. Cross-section bed profiles. C. birds eye view from the east of the gap in the shoal one month after the July 2014 bank failure. Depths in meters relative to Dutch ordnance datum, which is about present-day mean sea level. Maps, bed profiles and photo kindly provided by Edwin Paree and Marco Schrijver, Rijkswaterstaat Zee en Delta, Middelburg, The Netherlands. Note that the initial vertical failure scarp in the shoal was smoothed by waves and tidal currents, at the time the March 2015 laser altimetry was executed and the oblique photo was made.

2013, 2014; Mazières et al., 2014) support the occurrence of long-lasting turbidity currents in the immediate vicinity of the failure, which is difficult to explain in case of a liquefaction flow slide;

- Computational results of turbidity current velocities near the bed of a submarine canyon, obtained from a one-dimensional model in which breach growth is incorporated, show satisfactory agreement with quasi-steady flow conditions measured during a presumed breach failure event at the canyon head (Mastbergen and Van den Berg, 2003);
- Based on a literature survey of modern coastal sands, You et al. (2014) state that in the majority of the published cases the sands of coastal environments are dilative. Even sands that have been deposited very quickly in the inner bend of a channel and might be expected to behave contractant, may be susceptible to breaching within a few years after deposition: some inner bends

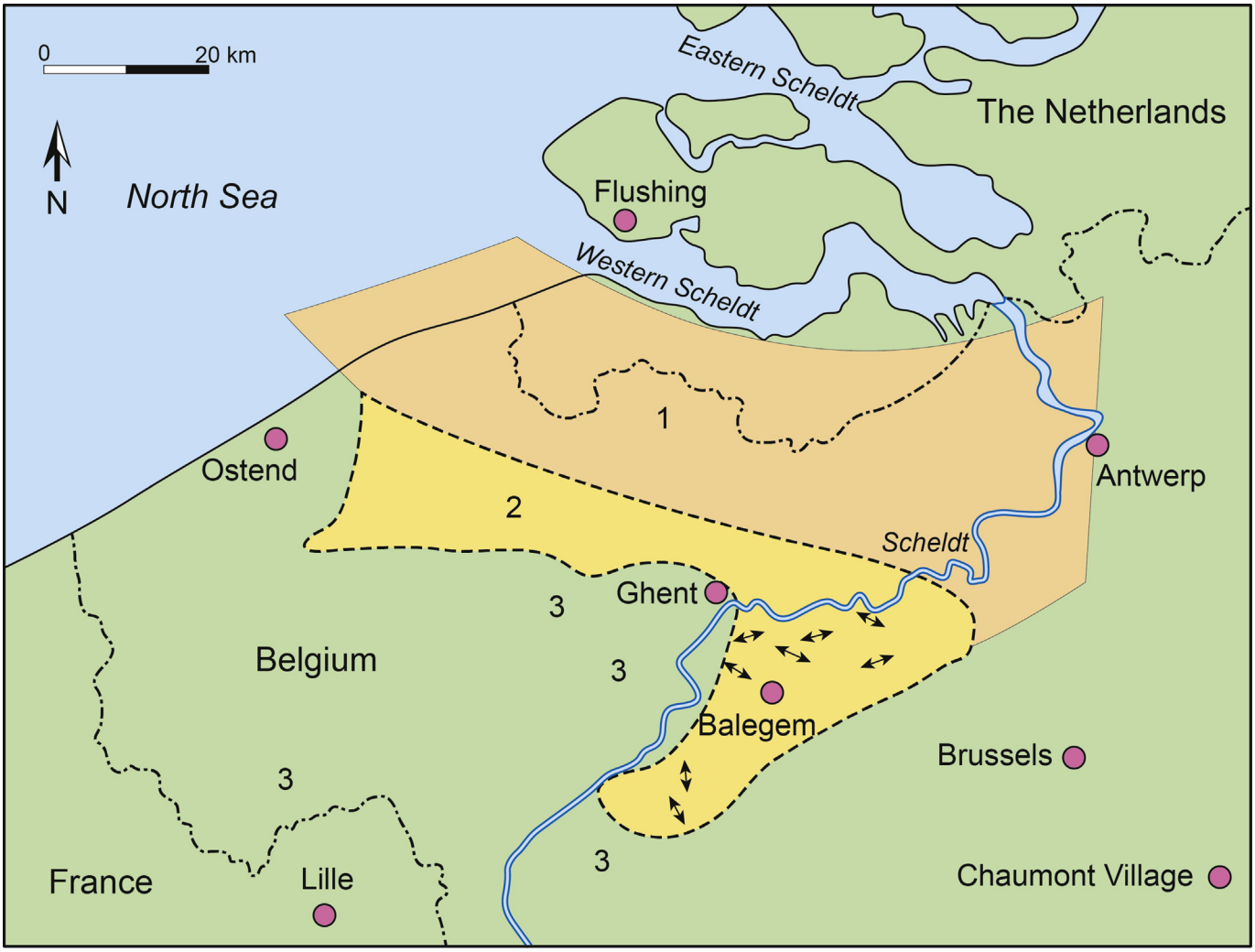

Fig. 2. Generalized map of the Vlierzele Sands in NW Belgium. The shape of the outcrop area is determined by present-day plateau areas (the original extent was larger, such as shown by the outliers); Balegem: location of the sand pit studied in this paper. 1. Subcrop; 2. Outcrop; 3. Outliers with occurrence of a few meters of Vlierzele Sands; 5. Short stripes near Balegem indicate tidal flow directions such as indicated by cross bedding. Tectonic dip is < 1° to the NNE. Dominant directions of the tidal flow (Houthuys, 1990).

Table 1
Main discriminating characteristics of massive-type sandstones and associated deposits recognized in this study.

Description	Nature of lower surface	Internal structures (disregarding structureless sand)	Interpretation[a]
Sheet-like massive-type sandbodies (SMS)	Undulose with localized cut and fill structures or non-erosional covering pre-existent bedform morphology	Near erosional base: spaced planar lamination may occur; near non-erosional base: some faint laminae possible; near top: some convolutions possible	high density turbidite by breach failure
Channel-like massive-type sandbodies (SMC)	Highly erosive with steep scours	Near erosional base: parallel spaced lamination, curving up the channel margins	high density turbidite by breach failure
Sheet-like packages of spaced planar lamination (SSL)	Plane erosive	Spaced planar lamination	high density turbidite by breach failure
Scoop- or sheet-like massive- type sandbodies (SL)	Undulose scouring	Convolutions, water escape structures	very clean sand debrite by liquefaction

[a] Density flow terminology following Talling et al. (2012).

of channels in the estuaries of the SW Netherlands and tidal inlets of Queensland, Australia, are well-known for their frequent occurrence of large bank failures, often repeated at almost the same locations (Wilderom, 1979; Beinssen et al., 2014). After a failure the original bank slope is restored in a few years and becomes again susceptible for a next breach failure. A well-documented example of such repeated failures is the inner bend of the Zuidergat channel in the Western Scheldt (Fig. 1). In a large field test executed in the same area (also indicated in Fig. 1), a bank failure that was triggered by dredging, turned out to be dominated by breaching (Mastbergen et al., 2016).

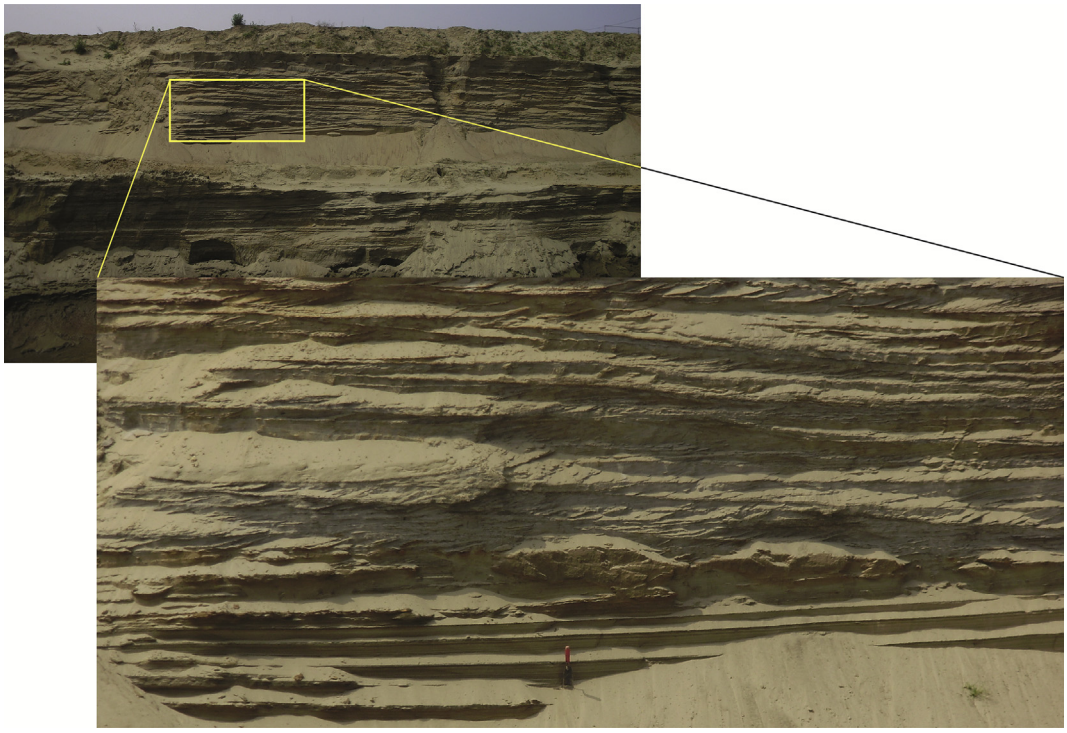

Fig. 3. Low angle planar lamination truncated by tidal crossbedding in the Balegem pit, Vlierzele Sands. Red hand grip of the trowel measures 11 cm. The truncation surface is about 30 cm above the trowel.

Fig. 4. Escape structures in a layer of spaced planar lamination.

- In liquefaction flow slide failures, where in contrast to a failure dominated by breaching a large mass of sediment is transported downslope in a very short spell, a tsunami may ensue, as reported e.g. by Harbitz et al. (2006). However, notwithstanding the fact that 1129 large bank failures were documented by Wilderom (1979) in the tidal channels and estuaries of the SW Netherlands, there are no reports of any tsunami ever observed in this area.

Inspired by his colleagues that collaborated in the breaching experiments in flumes at Delft Hydraulics, commissioned by the Dutch dredging industry, Torrey (1995) was the first to link natural bank failures with breaching. His study concerned bank failures of the lower Mississippi. It appeared that many of the failures, some of which involved more than a million cubic meters, occurred in dilative sands and therefore could not be ascribed to liquefaction, as supposed previously. At present, two decades later, breaching is recognized as an important failure mechanism and is incorporated in assessment rules for flooding safety in the Netherlands (Van Duinen et al., 2013), although in some very obvious cases, such as for instance the recurrent bank failures in the entrance of the Arcachon basin, France (Nedelec and Revel, 2015), breaching was still not recognized. Similarly liquefaction is still considered the main mechanism of large slope failures that produced massive sands in ancient deposits (e.g. Stow and Johansson, 2000). Now that it is clear that in present-day environments breaching rather than liquefaction is the main failure process in slopes of fine to medium sand, it is to be expected that the depositional products of bank failures in such sands also relate to failures dominated by breaching instead of liquefaction. An important implication is that by far most if not all large sandy bank failure related massive sands must represent structureless or faintly laminated intervals of turbidites.

In contrast to the well-known turbidites that are deposited under practically unconfined conditions in deep water environments, flow dynamics and depositional processes in turbidity currents produced by breach failures in channel banks are strongly influenced by the morphology of the channel. In a fluvial or estuarine channel, the turbidity current produced by a bank failure comes to a halt, which results in extremely rapid sedimentation. In the Vlierzele Sands, Eocene, Belgium, the only ancient estuarine deposit in which breach failure related phenomena are described so far, this resulted in massive sand layers that quite often bury part of a tidal dune landscape without any erosion (Van den Berg et al., 2002; Martinius and Van den Berg, 2011).

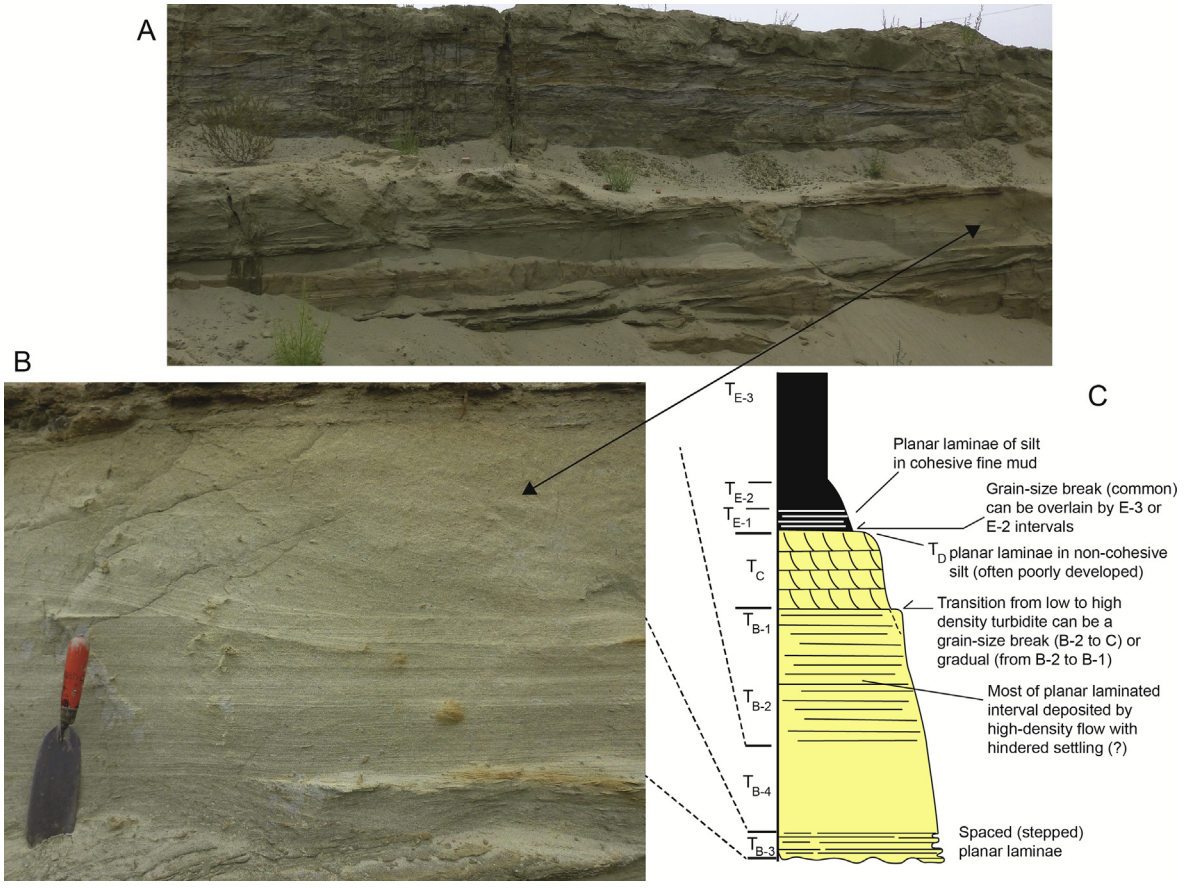

Fig. 5. A,B = Overview, detail massive sand layer in outcrop; C = Generalized turbidite sequence by Talling et al. (2012), slightly modified (see text).

Fig. 6. Detail of spaced planar lamination (position trowel Fig. 3).

3. Breach failure generated turbidites in the estuarine Vlierzele Sands, Eocene, Belgium

The Vlierzele Sands (late Lower Eocene, member of the Gentbrugge Formation, Steurbaut et al., 2016) consist of a 10–20 m thick unconsolidated body of fine glauconiferous siliciclastic sand (100–200 μm) found at or slightly below the land surface in northern and western Belgium (Fig. 2). The estuarine channel nature of at least part of the Vlierzele Sands is demonstrated by 1) some deep channel incisions into the underlying, clayey Lower Eocene succession (Mostaert, 1985; De Batist, 1989; De Batist and Versteeg, 1999), 2) the presence of some lignitic deposits in the upper part of the Vlierzele Sands (Gulinck and Hacquaert, 1954) and above all 3) the mud draped cross-bedding present in the upper part that reveals many characteristics of inshore tidal channels (Van den Berg et al., 1998). In exposures in several sand pits near Balegem, massive sand layers were found intercalated between inshore tidal cross-bedding. These poorly structured beds were first thought to have originated from dense storm-caused sand suspensions (Houthuys and Gullentops, 1988; Houthuys, 1990), but later reinterpreted as products of breach failures (Van den Berg et al., 2002). The massive sands occur both in non or slightly erosional sheets and steeply incised channel fills, termed sheet-like massive sandstone element (SMS) and channel-like massive sandstone elements (SMC), respectively by Martin (1995) and Martin and Turner (1998), for much similar sandbodies in the Fell Sandstone discussed in the next paragraph. For convenience these acronyms are adopted in this paper. The main characteristics of the massive sandstone facies and associated elements discussed in this paper are described below and summarized in Table 1. The massive sandstones range in thickness from a few decimeters up to occasionally 4 m and generally are truncated by tidal cross-bedding (Fig. 3). Although seemingly structureless, they generally contain some solitary faint laminae or horizons with a slightly different colour due to subtle changes in very small admixtures of organic material, heavy minerals and mud, that demonstrate that they were deposited incrementally layer by layer.

Sheet-like massive-type sandbodies (SMS). These elements generally have some faint parallel lamination at their base. Some of the SMS elements cover trains of completely preserved dune formsets constituting 3D patterns that may extend over more than several hectares (Houthuys, 1990).

Channel-like massive-type sandbodies (SMC). In contrast to the non-erosional, sheet-like massive sand bodies, massive sands are also present in fills of steeply scouring channels, with steep sides, up to vertical in places. Generally near the basal erosion surface some faint lamination is present that curves up the sides of the channel scour, sometimes with some erosional disconformities (See Fig. 9 in Van den Berg et al., 2002).

Sheet-like packages of spaced planar lamination (SSL). Ongoing mining in the Balegem pit re-exposed several sheet-like packages of low-angle plane planar lamination (SSL), visually showing a rather wide spacing between individual strata, that had before been interpreted as being produced by strong wave action (Houthuys, 1990). However, they were found in a relatively deep depositional position with respect to the other types of deposits and intercalated in massive sands (See Fig. 5.11 in Houthuys, 1990). Some rare animal escape structures (Fig. 4) demonstrate that the deposition rate of the planar lamination was very high. In some of the planar laminated layers the lamination fades upwards into a massive sand (Fig. 5). The latter observation discloses the type of the lamination as so-called spaced or stepped planar lamination (Hiscott, 1994; Talling et al., 2012; Sumner et al., 2012) that corresponds to the T_{B-3} division as the lowermost part of the Bouma sandy high-density turbidite succession proposed by Talling et al., 2012 (Fig. 5C), or the S2 division in Lowe's succession (Lowe, 1982). Spaced planar lamination is characterized by 0.5–15 cm thick strata, which in deposits with a wide range of grainsizes show alternation of coarser and finer grainsize (Lowe, 1982). Although the mechanism of sorting producing the grainsize differentiation is still not clear, there is consensus that this type of lamination results from cycles of collapse and regeneration of a traction carpet beneath a decelerating high-density current (Hiscott and Middleton, 1980; Lowe, 1982; Sumner et al., 2008; Talling et al., 2012; Malgesini et al., 2015). In the well sorted overall fine-grained sand of the Vlierzele Sands, the spaced planar stratification is accentuated by an alternation of somewhat darker and lighter layers due to apparent mineralogical sorting of glaucony grains (Fig. 6). As grain-size variation in spaced planar lamination is not an apparent characteristic in deposits of well-sorted sands, in this

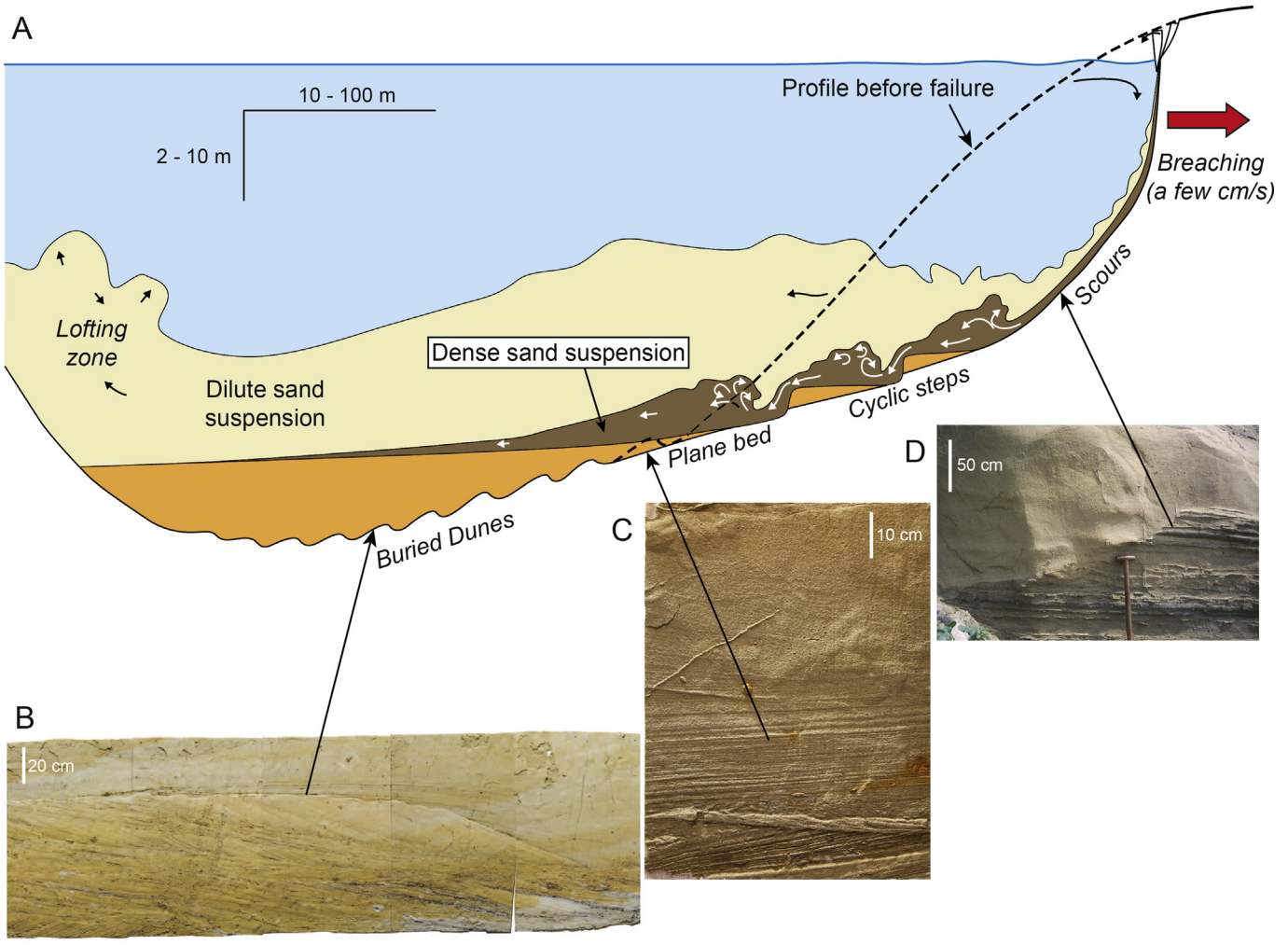

Fig. 7. Schematic overview of a turbidity flow from an ongoing breach failure in a channel, related bedforms and sedimentary structure. In reality, the number of dunes and cyclic steps may be an order of magnitude larger. A: Cross-section of channel bend, inner bank is to the right (partly after Van den Berg et al., 2002); B: Dune formset buried by massive sand with at the base some faint lamination paralleling the dune (Martinius and Van den Berg, 2011); C: Spaced planar lamination merging upwards into faint lamination followed by massive sand (lacquer peel made at location Fig. 5B); D: Scour filled with massive sand (Van den Berg et al., 2002).

paper this term is used in a strictly descriptive sense. Within a package of spaced planar lamination some erosional discontinuities may be present (Fig. 5B). Flume experiments indicate that spaced planar lamination in fine sands turns into structureless sand at aggradation rates larger than 0.44 mm/s (Sumner et al., 2008). The massive sands in the Vlierzele Sands therefore refer to very high sedimentation rates.

Scoop- or sheet-like massive-type sandbodies (SL). These massive beds are characterized by the presence of highly contorted bedding. In the Vlierzele Sands such sandbodies were not encountered. In the examples discussed in this paper only one SL element was found in one of the outcrops of the Fell Sandstone discussed later in this paper.

In the center of the Vlierzele tidal channel, where the turbidity current decelerated very quickly because of the confinement of the channel, very high sedimentation rates started directly with the arrival of the turbidity current leaving the pre-event morphology undisturbed. This explains the preservation of dune formsets. The deeply scouring channels at the base of the SMC units are considered to be carved in the lower part of channel banks by the energetic turbidity flow downslope of the retrograding breach failure. Fig. 11 in Van den Berg et al. (2002) illustrates these extremes in flow strength and deposition in a model of the morphology and deposits produced directly after a breach failure event in a deep tidal or river channel. In a further elaborated version, shown here in Fig. 7, a flat area (Fig. 7C) is inferred, where spaced planar lamination is produced. This zone fits well in between the zone of erosional scours and cyclic steps near the failure (Fig. 7D) and the rapid deposition area in the channel center (Fig. 7B): moderate, not channelized erosion followed by a moderate deposition rate.

In the turbidite sequence presented by Talling et al., 2012, the structureless to faintly laminated layer is classified T_A. Recent advances in understanding indicate that structureless T_A units – in coarse grained turbidites characterized by a coarse-tail normal grading - reflect deposition directly behind a hydraulic jump (Postma et al., 2009). In the sequence of Talling et al. (2012) spaced lamination (T_{B-3}) merges upwards gradually into structureless sand (T_A), indicating a gradual transition of flow and sedimentation conditions instead of a sudden hydraulic jump-related switch. Therefore we changed the classification label of this unit into T_{B-4} (see Fig. 5C), the almost structureless "frictional traction carpet facies" as defined and described by Postma et al. (2014) and Postma and Cartigny (2014). A remarkable consequence is that unit T_A, the lowermost part of the classical 5-partite Bouma sequence, is lacking in the sequence presented by Talling et al. (2012; Fig. 5C).

In the very steep slope of a retrograding wall in a breach failure, the turbidity current quickly becomes supercritical and may probably reach internal Froude number values slightly above 2.8, where Kelvin-Helmholtz billows form that strongly enhance mixing with the overlying fluid (Mastbergen and Van den Berg, 2003). As a result, a dilute sediment suspension layer will quickly develop on top of a dense near-bed high-density turbidity current (Fig. 7). It was speculated by Van den Berg et al. (2002) that the supercritical turbidity current passes to subcritical through a series of hydraulic jumps and related upslope migrating cyclic steps. Although so far no depositional evidence of the presence of such upper flow regime bedforms was found in the Vlierzele Sands, it is nevertheless

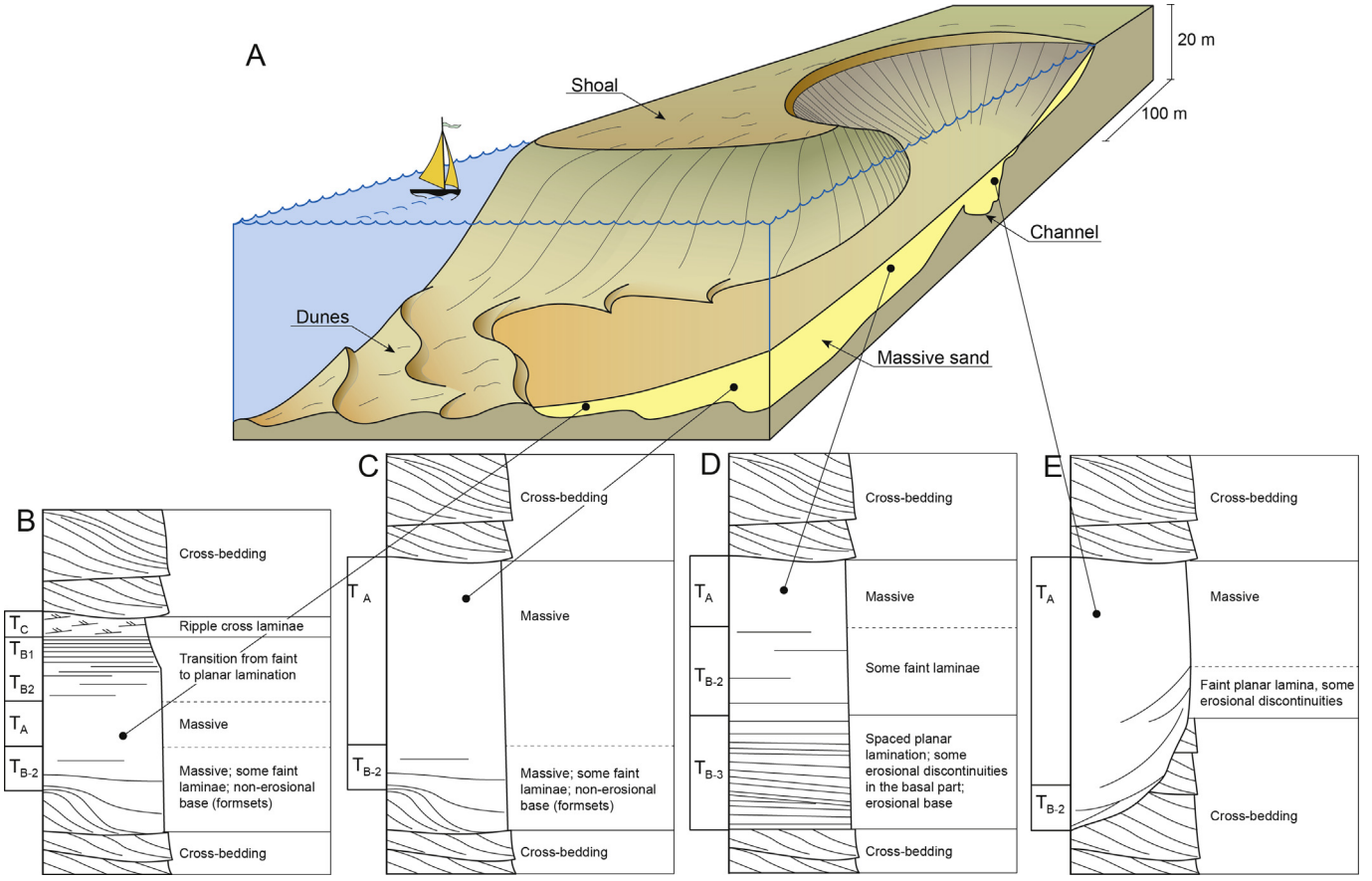

Fig. 8. Reconstruction of morphology and deposits produced after a breach failure event in a deep tidal or river channel. A: post-event morphology; B–E: breach failure generated turbidite after burial by fluvial or tidal cross-bedding (partly after Van den Berg et al., 2002).

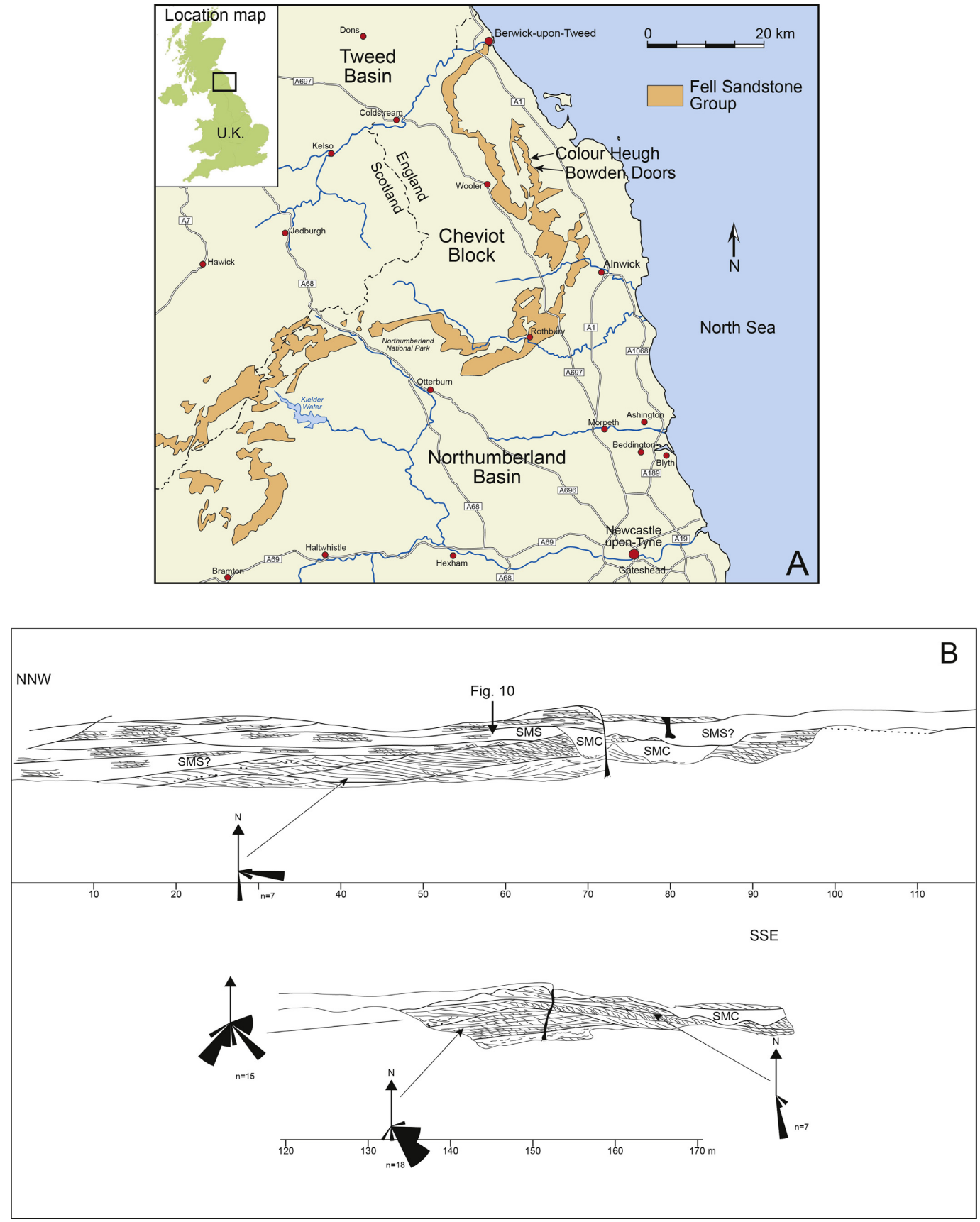

Fig. 9. The Fell Sandstone: A. The outcrop of the Fell Sandstone Group in the Northumberland Basin, and the location of Bowden Doors and Colour Heugh Crags (after Turner and Monro, 1987); B and C. Simplified line drawings of the section exposed at Colour Heugh and Bowden Doors escarpments respectively (modified after Martin, 1995).

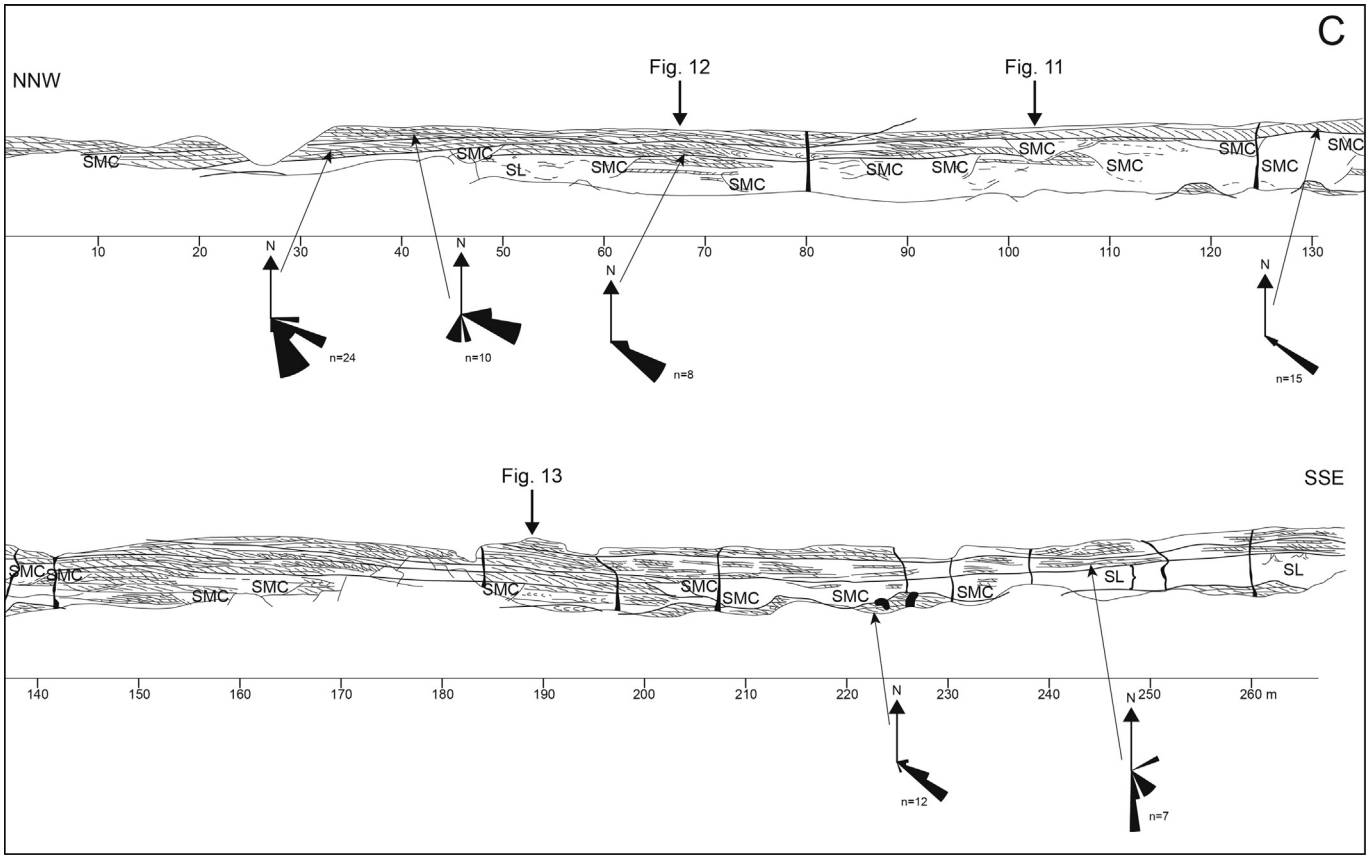

Fig. 9. (*continued*).

believed that cyclic steps were formed, because, as mentioned earlier in this paper, in multibeam images downstream of suspected breach failures generally cyclic steps are observed. The area where cyclic steps might form is erosive as it follows the retrograding breach failure. This may explain the absence of hydraulic jump related T_A units in turbidites in the studied outcrops of the Vlierzele Sands. While the lower layer of dense suspension loses sand to the overlying dilute suspension, it gains sediment from erosion of the bed. Numerical models are currently not able to realistically model dense basal flows with densities over 10% volume by concentration, where grain-to-grain interaction and hindered settling are the dominant sediment supporting mechanisms (Clare et al., 2015). We speculate that over a field of cyclic steps the dense basal layer has a more or less constant thickness averaged over the bedforms, as suggested in Fig. 7. This statement, also suggested by drawings in Van den Berg et al. (2002), Cartigny et al. (2011) and Postma and Cartigny (2014), is motivated by the fact that multibeam echo sounder pictures of cyclic step patterns after a short initial track of growth often do not show a downstream change in bedform dimensions (e.g. Paull et al., 2013; Smith et al., 2005, 2007; Casalbore et al., 2014; Cartigny et al., 2017; Hughes Clarke, 2016) that can be expected if the formative flow would increase in thickness downstream (Cartigny et al., 2011).

At the distal part, away from the breach failure, the turbidity flow is blocked by the opposite bank and therefore decelerates quickly in the channel. This blockage explains the lofting assumed in Fig. 7. Sand grains settle from the dilute suspension down into the dense sublayer, where hindered settling reduces the fall velocity of the grains. This process sharpens the interface between the dilute and dense suspension layer and reduces the velocity of its collapse, which is why we think that it will spread over an area of the order of 5–50 ha before disappearing completely. Thereafter the sedimentation rate will be very much reduced, the more so as part of the plume of dilute suspension is transported away with the tidal or fluvial flow. This explains the formation of a planar laminated T_B or, aided by the presence of a tidal current, a ripple-laminated T_C interval as drawn in Fig. 5C. Numerous pre- and post failure event soundings in the tidal channels of the SW Netherlands demonstrate that the total thickness of the turbidite

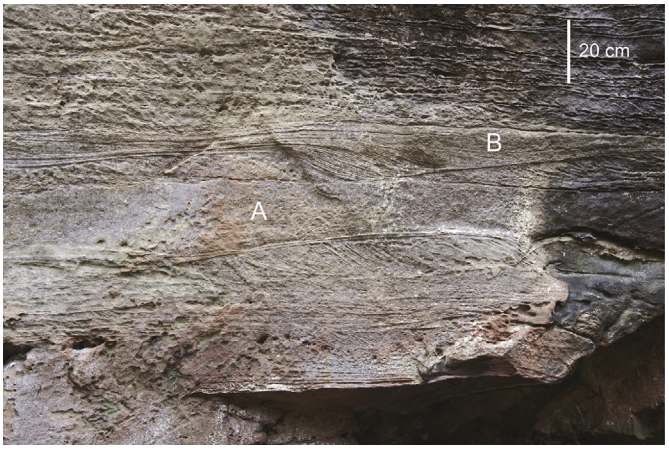

Fig. 10. Two massive-type SMS sandbodies (A and B) covering dune formsets. Note the presence of some faint lamination at the base of the structureless sand, especially for the uppermost unit. Colour Heugh, for location see Fig. 9B.

directly after its deposition can easily surpass 10 m (Wilderom, 1979). Such a deposit constitutes an obstacle for the tidal flow through the channel and the main part of it may therefore erode quickly, leaving only the lowermost part a chance to preserve. In Fig. 8, an impression is sketched of a post event morphology and the related turbidite as it becomes sandwiched in between cross-bedded units in the months or years after the event. Unless the channel is abandoned by the flow, only near the thin edges of the lens-shaped turbidite, where erosion by tidal or fluvial flow is much less, the upper part of the turbidite has a chance to preserve (Fig. 8B). As soon as the rapid aggradation of the channel by the sustained sand supply from the breach failure reaches the level of the steep scour gully that guides the turbidity current, erosion in this scour switches to increasingly rapid deposition. This can explain why deposition that often started with spaced planar lamination was followed soon by structureless sand (Fig. 8D).

All evidence put together, it is rather obvious that breach failure events are the origin of the massive sands in the Vlierzele Sands. Three breach failure related sediment architectural elements can be discriminated: (1) channel-like (SMC), (2) sheet-like (SMS) massive sandbodies and (3) sheet-like bodies that consist of a package of spaced planar lamination (SSL). All these three elements are the product of turbidity currents generated by breaching and fit in the model of Fig. 7 that explains their sedimentary characteristics and shows how these architectural units are positioned with respect to each other and to the location of the breach failure.

4. Breach failure generated turbidites in outcrops of the fluvial Fell Sandstone, Lower Carboniferous, England

The Lower Carboniferous Fell Sandstone (Mid Dinantian) comprises up to 350 m of sublitharenite, subarkose and quartz arenite. The sandstone deposited in the rapidly subsiding Northumberland Trough by what is considered a large-scale sandy braided river system, which culminated in a fluvially dominated delta in the west of the trough (Monro, 1986; Turner and Monro, 1987; Martin, 1995; Martin and Turner, 1998). The sands are generally fine, with a median diameter of 135 μm and deposited in channels that according to Martin and Turner (1998) were 12–18 m deep at bankfull stage. The main outcrops where fluvial channel deposits are exposed and studied by the authors mentioned above are known as *Bowden Doors* and *Colour Heugh* (also named *Back Bowden Doors*). As part of the present analysis, these outcrops, sketched in Fig. 9, were revisited.

The Bowden Doors and Colour Heugh escarpments show very well exposed fluvial cross bedding. Inserted in this unidirectional cross bedding all three breaching-related architectural units distinguished in the Vlierzele Sands are present. In addition to the SMS and SMC elements in Bowden Doors, a third massive sandbody was identified by Martin (1995) and Martin and Turner (1998) that shows some contorted bedding due to liquefaction (Fig. 9C, marked by "SL"). The fact that original primary structures have not completely disappeared indicates that the liquefaction caused only

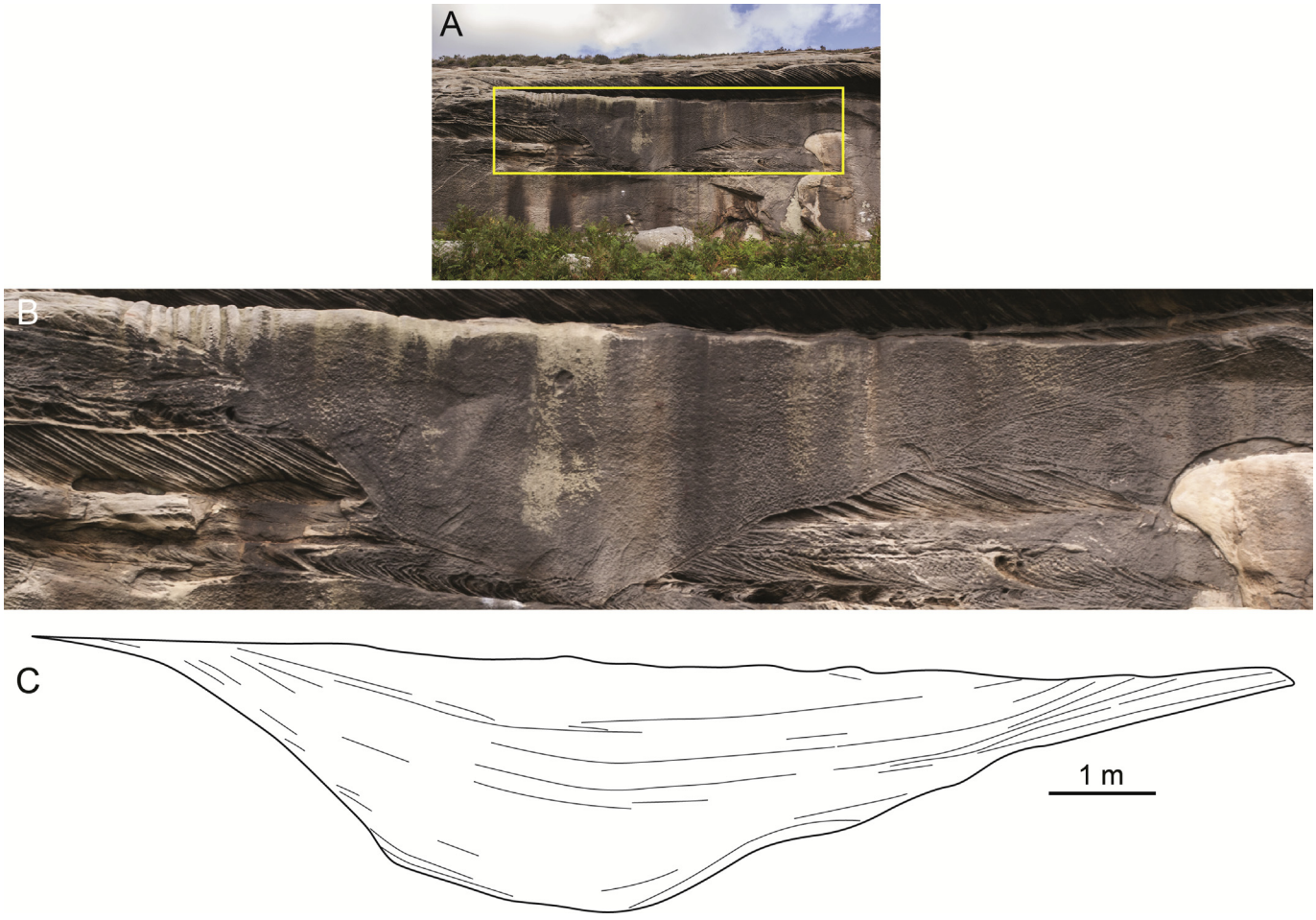

Fig. 11. Faint laminae and beds documenting the flattening of the channel during the process of channel fill in a cross-section of a SMC sand body, Bowden Doors, location known by climbers as "The Wave", for location see Fig. 9C. The sandstone scarp (A) is 6,5 m high. Photo courtesy John Dalrymple.

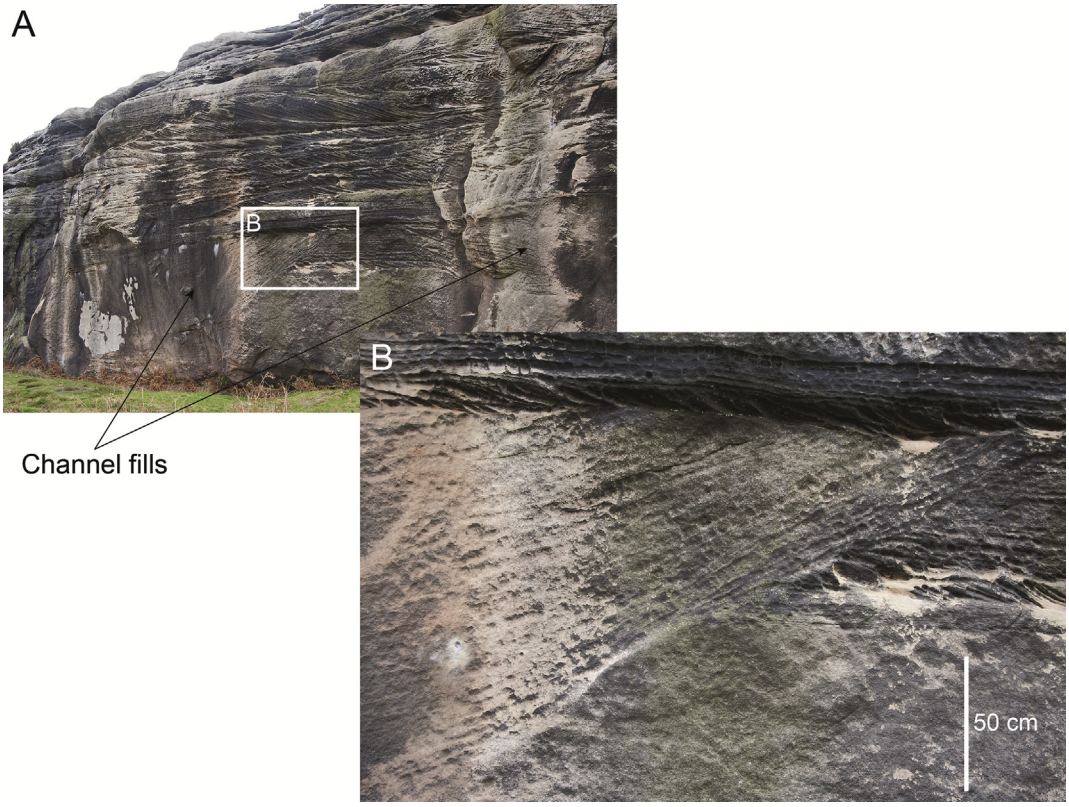

Fig. 12. SMC sandbodies filled with spaced lamination. Bowden Doors escarpment, location known as "Poverty", see Fig. 9C.

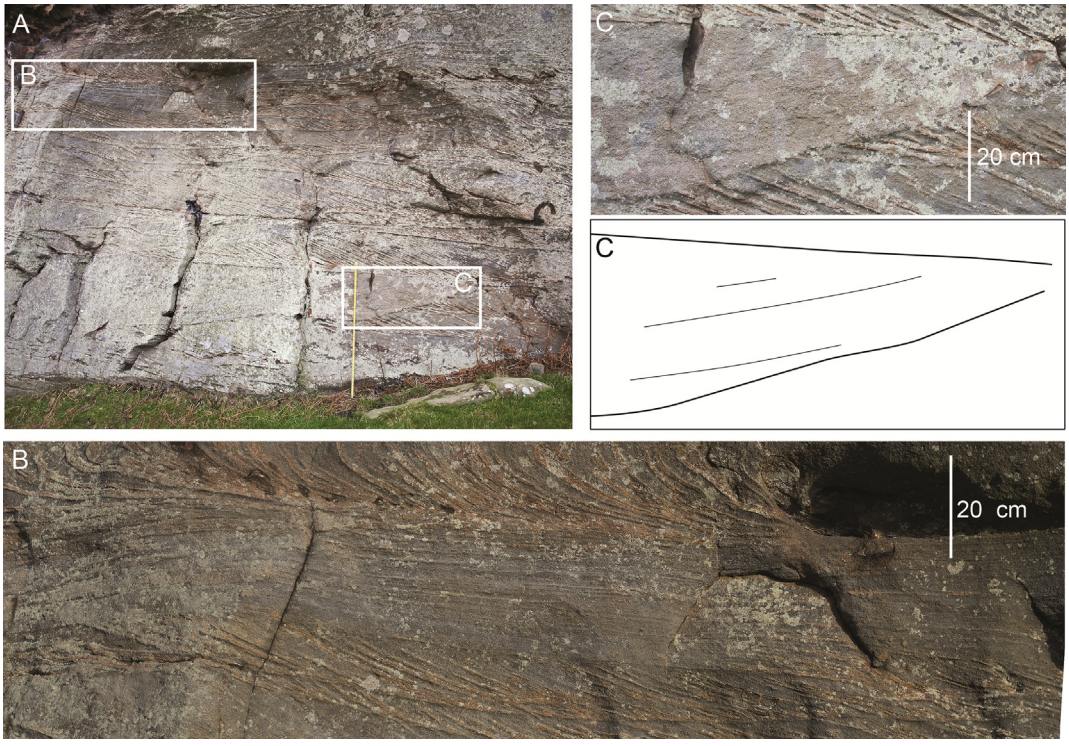

Fig. 13. Two different breaching related architectural elements inserted in fluvial cross-bedding. A. Overview; B. SSL body with spaced planar lamination; C. SMC massive-type unit with some faint laminae. Photos courtesy of John Dalrymple. Bowden Doors escarpment, location known as "Runnel", see Fig. 9C.

a small displacement of the sand mass involved.

Like in the Vlierzele Sands, some of the massive SMS sandstone units rest on an undisturbed morphology of dune formsets (Fig. 10). The Fell Sandstone escarpments are aligned more or less parallel to the direction of the fluvial channels. Therefore, the SMC sandstone units that run perpendicular to this, are only seen in cross-section. In all previous studies of the Bowden Doors and Colour Heugh escarpments, the massive sandstone above the lamination that hugs the channel margin was described as apparently structureless. However, careful examination shows that often some vague bedding or some faint laminae are present (Fig. 11), demonstrating that these massive sands were laid down incrementally layer by layer and not *en masse* by a debris flow as suggested by previous workers (Monro, 1986; Turner and Monro, 1987; Martin, 1995; Martin and Turner, 1998). Like in the Vlierzele Sands at the base and margins of many of the SMC units, generally some faint centimeter scale lamination is found. We agree with Martin (1995) and Martin and Turner (1998) that this spaced lamination is the result of frictional freezing. Dewatering structures preserved in the upper portion of some of the SMC and SMS elements (Martin and Turner, 1998) indicate the swift aggradation that caused the absence of primary sedimentary structures in the sand above the faintly laminated beds. In some of the SMC units, this lamination extends over a larger distance from the erosive incision surface and may even be present over the whole preserved channel fill (Fig. 12). Apparently, in such cases the accumulation rate did not surpass the critical limit for the disappearance of lamination.

The fluvial cross bedding is often organized in descending cosets (Fig. 12A). Such structures are explained by small fluvial dunes descending the lee-sides of a larger dune and often reflect hysteresis in dune adaptation during the falling discharge stage in a deep river (Allen and Collinson, 1974; Martinius and Van den Berg, 2011; Reesink and Bridge, 2011). Intercalated between the fluvial cross-beds in the Bowden Doors escarpment, a slightly undulating to horizontal laminated layer was found that was not described in previous studies (Fig. 13). Because of the large water depth such as testified by the cross-bedded units, an upper plane bed origin is unlikely, and, in view of the wide spacing between the laminae, this unit is interpreted as representing the laminated third architectural element (SSL) of breach failure related deposits that is formed in a zone of plane beds close to the failure (Fig. 7). This architectural element may be present at more locations in the studied escarpments, as they have not systematically been inspected for their presence.

An alternative interpretation for SSL bodies and SMS elements with an erosional base is that they refer to hyperconcentrated fluvial slurry flows. Actually, some of the SMS units were attributed to such flows by Martin and Turner (1998). Although the situation of the Fell Sandstone river in a delta makes such high energetic flows unlikely, it is not easy to exclude a fluvial slurry flow origin, simply because a turbidity current generated by breaching is also a hyperconcentrated flow. The main difference is that flow strength in a channel during aggradation by a breach failure derived turbidite is low, whereas hyperconcentrated streamflows have a high velocity. This high flow strength may be documented in sandy deposits of hyperconcentrated streamflows by heavy mineral

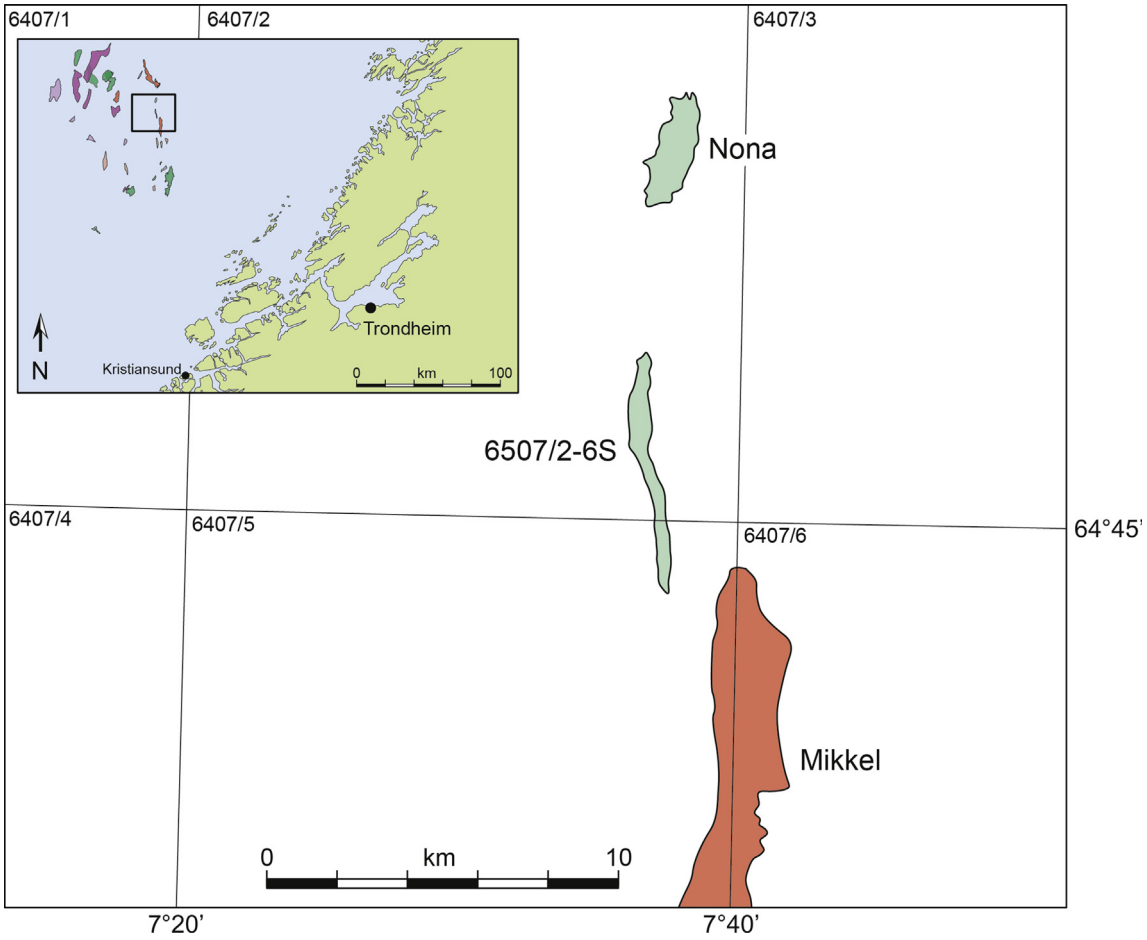

Fig. 14. Location map of the Flyndretind field northwest of Trondheim.

concentrations (Dilliard et al., 1999), pebble strings resting on scoured surfaces left by erosional episodes and grainsize differences over small distances (Dilliard et al., 1999; Macías et al., 2004). All these characteristics of hyperconcentrated streamflows are lacking in the SSL and SMS elements in the studied outcrops of the Fell Sandstone, which supports their breach failure related origin.

5. Possible breach failure origin of massive sands in cores of the Norwegian Continental Shelf

5.1. The Lower Jurassic Tilje formation

The Pliensbachian to Toarcian Tilje Fm (Dalland et al., 1988) formed in a mixed-energy tide-dominated deltaic environment in a relatively shallow-water semi-enclosed basin. A significant fraction of the sediment delivered to the deltas and associated embayments consisted of mud and silt, and, as a result, the reservoir intervals are composed of sedimentary packages that are strongly heterolithic and show a bimodal grain-size distribution (Van de Weerd, 1996; Martinius et al., 2001; Ichaso and Dalrymple, 2014; Ichaso et al., 2016). Deposition took place in the Halten–Trøndelag Basin that encompassed the Halten Terrace and the Trøndelag Platform. This coast-parallel rift-generated basin became the locus of the Jurassic seaway that was approximately 1500 km long and 250 km wide (Gjelberg et al., 1987; Doré, 1991; Brekke et al., 2001). Initially during the Lower Jurassic, this relatively shallow seaway, with a complex palaeogeography and serrated coastline, was semi-enclosed and only connected to the Boreal Ocean in the north. Later during the Lower Jurassic, an opening developed also in the south to the Tethys Ocean. Subsidence rates varied across the Halten–Trøndelag Basin and the Tilje Fm reaches a maximum thickness of approximately 300 m in areas along active faults. The formation is divided into two major third-order stratigraphic sequences (Martinius et al., 2001). Across the Halten Terrace, the lower sequence is formed by sand-dominated, mostly aggradationally stacked parasequences consisting of heterolithic channel fill, tidal bar, mouth-bar, delta-front and in places prodeltaic deposits. Depending on changes in direction and magnitude of the main fluvial discharge, distributaries that became (temporarily) disconnected from the fluvial source transformed into inshore tidal basins, thereby changing the energy balance from fluvial-dominated to tide-dominated.

The cored sandstone containing the almost structureless homogeneous sandstone interval in Flyndretind (Figs. 14 and 15) is almost 19 m thick and formed by well to very well sorted, rounded to well-rounded very fine-grained sandstone. The basal 17 m is homogeneous, appears massive, and is largely unstructured with faint lamination occurring in approximately 20% of the interval (Fig. 14). Particularly in the basal 3.5 m of the cored section a number of faintly laminated sets have spaced lamination with individual laminae of up to 5 cm thick (Fig. 16). At a few locations, small (1–10 mm long), flat (1–2 mm thick) and parallel oriented silty mudstone clasts occur (Fig. 17). The uppermost 2 m are formed by very well-rounded and sorted, low-angle parallel laminated sandstone with set thicknesses of 10 mm–12 mm containing abundant very small (less than 1 mm) organic particles and diffuse organic material (Fig. 18). The amount of organic particles increases upward from a few to abundant giving the impression of successive thin dense lags. The top of the unit is muddy with thin layers of up to 5 cm long and 6 mm thick coal fragments.

This unit is overlain by a 17.5 m thick, cross-stratified, well to very well-rounded and sorted sandstone unit with abundant bidirectional current structures. Preserved cross-stratified set thicknesses vary between 8 and 15 cm. Double mud drapes and organic particles occur abundantly in the upper 7 m (Fig. 19A and B). The uppermost 2 m is formed by thinner sets (up to 10 cm thick) with abundant fluid mud layers and pervasive bidirectionality with an increasing amount of coal fragments; bivalve resting traces, *Planolites* and *Teichicnus* are common (Fig. 19C and D).

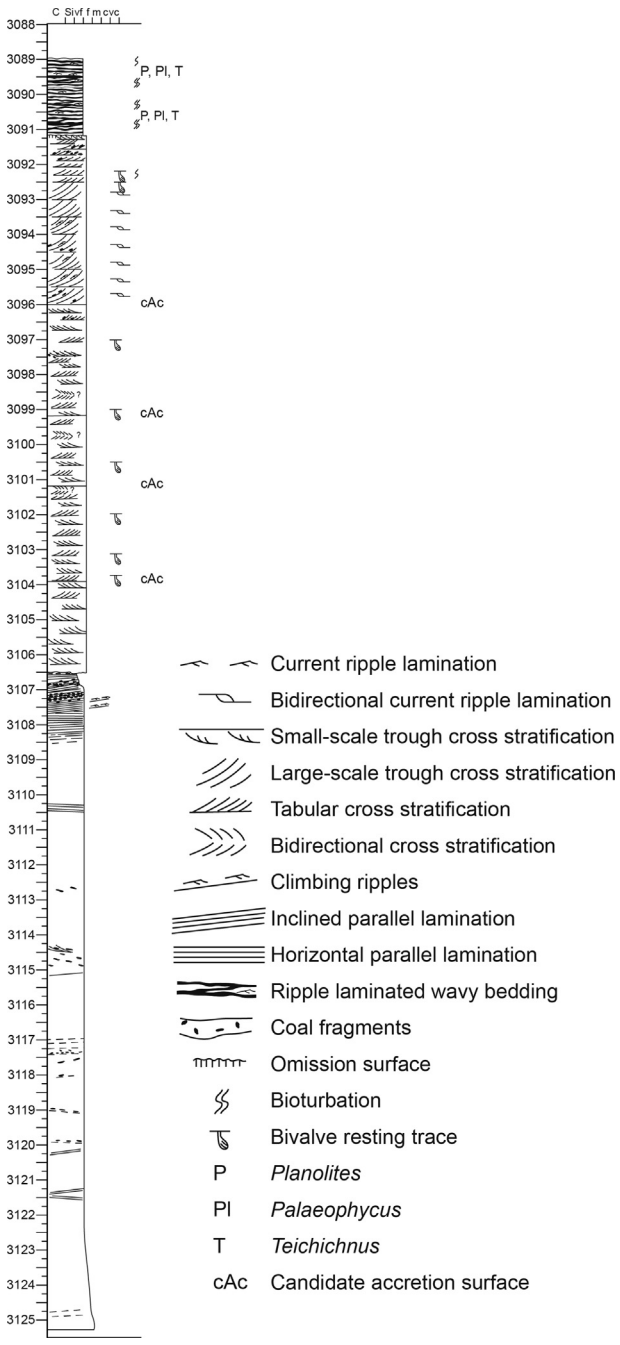

Fig. 15. Core description of the lower part of the Tilje Fm in Flyndretind.

The gamma-ray (GR) log for this cored part of the boring reflects well this subdivision in two units (Fig. 20) as indicated by the higher GR readings interpreted to reflect a higher degree of mudstone in the upper unit. It also illustrates that the lower unit is significantly thicker than the cored interval alone and continues for 18 m stratigraphically downwards from the base of the core. The lowermost 4 m (section 3149 to 3145; Fig. 20) show the lowest GR readings and is interpreted to contain the least amount of mudstone.

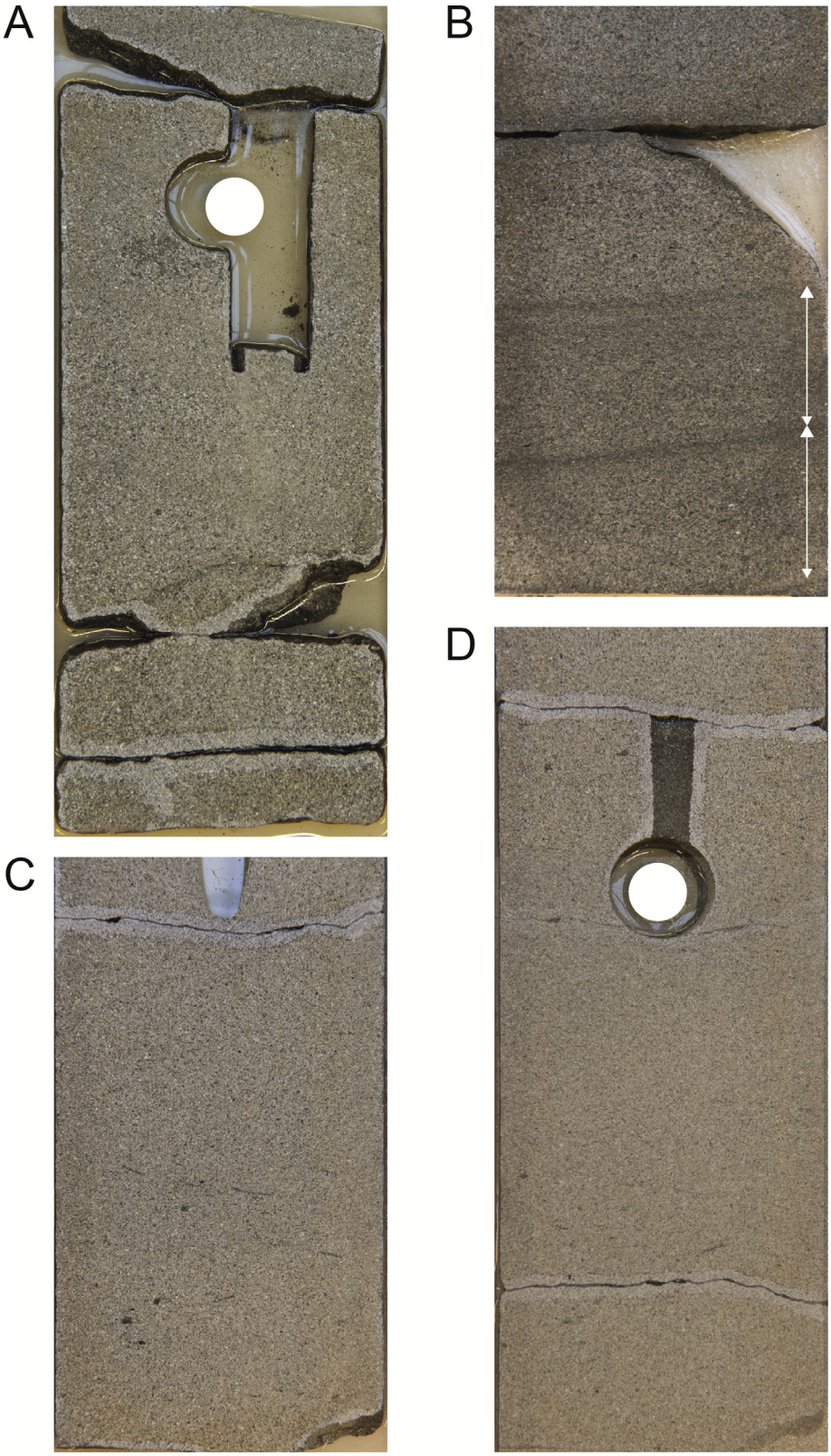

Fig. 16. A–D: Core examples of faintly laminated sets with spaced lamination (see double-sided arrows in B) with individual laminae of up to 5 cm thick (Tilje Fm, Flyndretind field). Core width is 9 cm. A: 3125,2 m; B: 3124.9 m; C: 3122.9 m; D: 3122.5 m (see also Fig. 15).

The in total 54.5 m thick sedimentary succession is interpreted as genetically related containing three main intervals. The lowermost (non-cored) 4 m are interpreted to have been formed as channel floor deposits in a probably large and active tidal channel in an estuary. This interval is overlain by the homogenous, 33 m thick sandstone interval, interpreted as the product of multiple

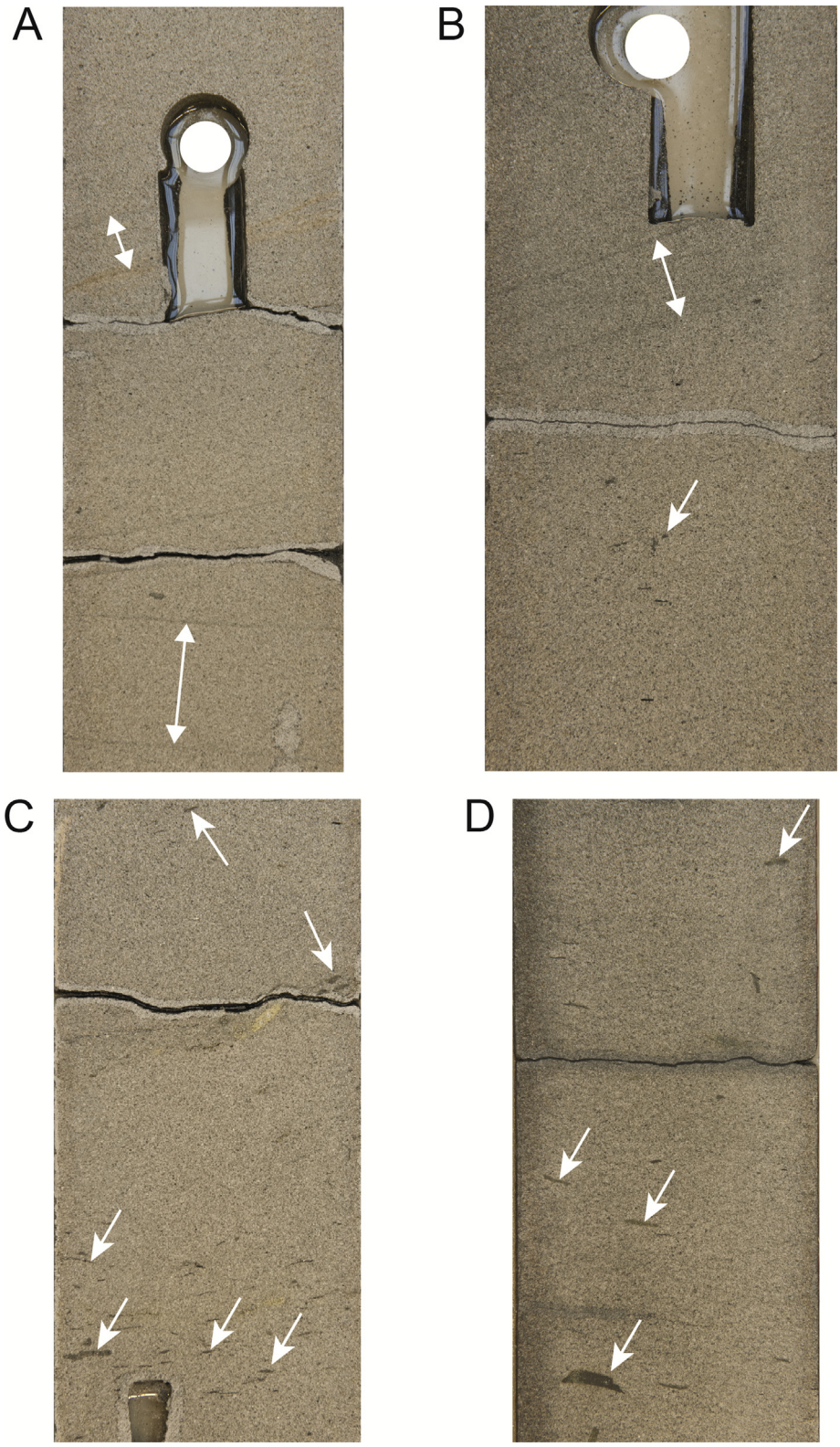

Fig. 17. A–D: Examples of small (1–10 mm long), flat (1–2 mm thick) and parallel oriented silty mudstone clasts, shown by arrows (Tilje Fm, Flyndretind field). Double-sided arrows are like in Fig. 16. Core width is 9 cm. A: 3120.35 m; B: 3120.30 m; C: 3117.45 m; D: 3114.50 m (see also Fig. 15).

turbidites in the channel each originated by a breach failure in the channel margin (either a tidal channel bank or the edge of a large tidal bar within the tidal basin; cf. Wilderom, 1979). This deposit can be classified as the fill of a deep scouring tidal channel analogous to the massive sand facies in the Vlierzele Sands described above (Fig. 8, situation D). Thin intervals of small muddy siltstone and coal pebbles are interpreted to indicate a (probably minor) degree of erosion of the top of the preceding breach failure

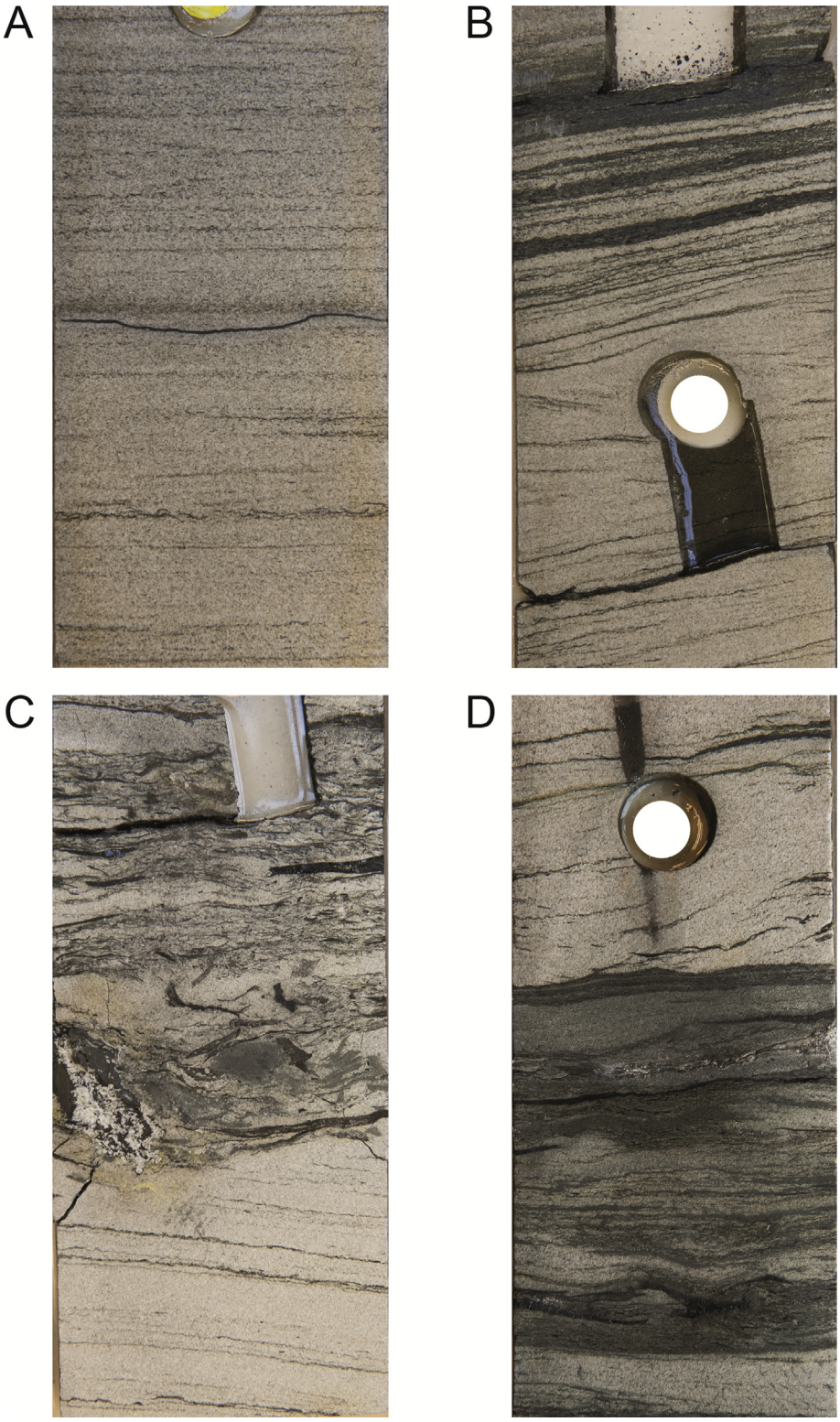

Fig. 18. A–D: Examples of very well-rounded and sorted, low-angle parallel laminated sandstone with set thicknesses of 10 mm–12 mm containing abundant very small (less than 1 mm) organic particles and diffuse organic material (Tilje Fm, Flyndretind field). Core width is 9 cm. A: 3107.80 m; B: 3107.15 m; C: 3106.85 m; D: 3106.70 m (see also Fig. 15).

deposit. The upper 17.5 m thick unit is interpreted as a tidal bar with (inter)tidal flat deposits at the very top. It must be kept in mind that although breaching rather than liquefaction is the main failure process in slopes of clean sand, for units without some faint lamination or a spaced planar laminated lower part, a (multiple) debris flow origin cannot be ruled out completely.

5.2. The Lower Jurassic Nansen formation

The Hettangian to early Sinemurian Nansen Fm (Lower Jurassic;

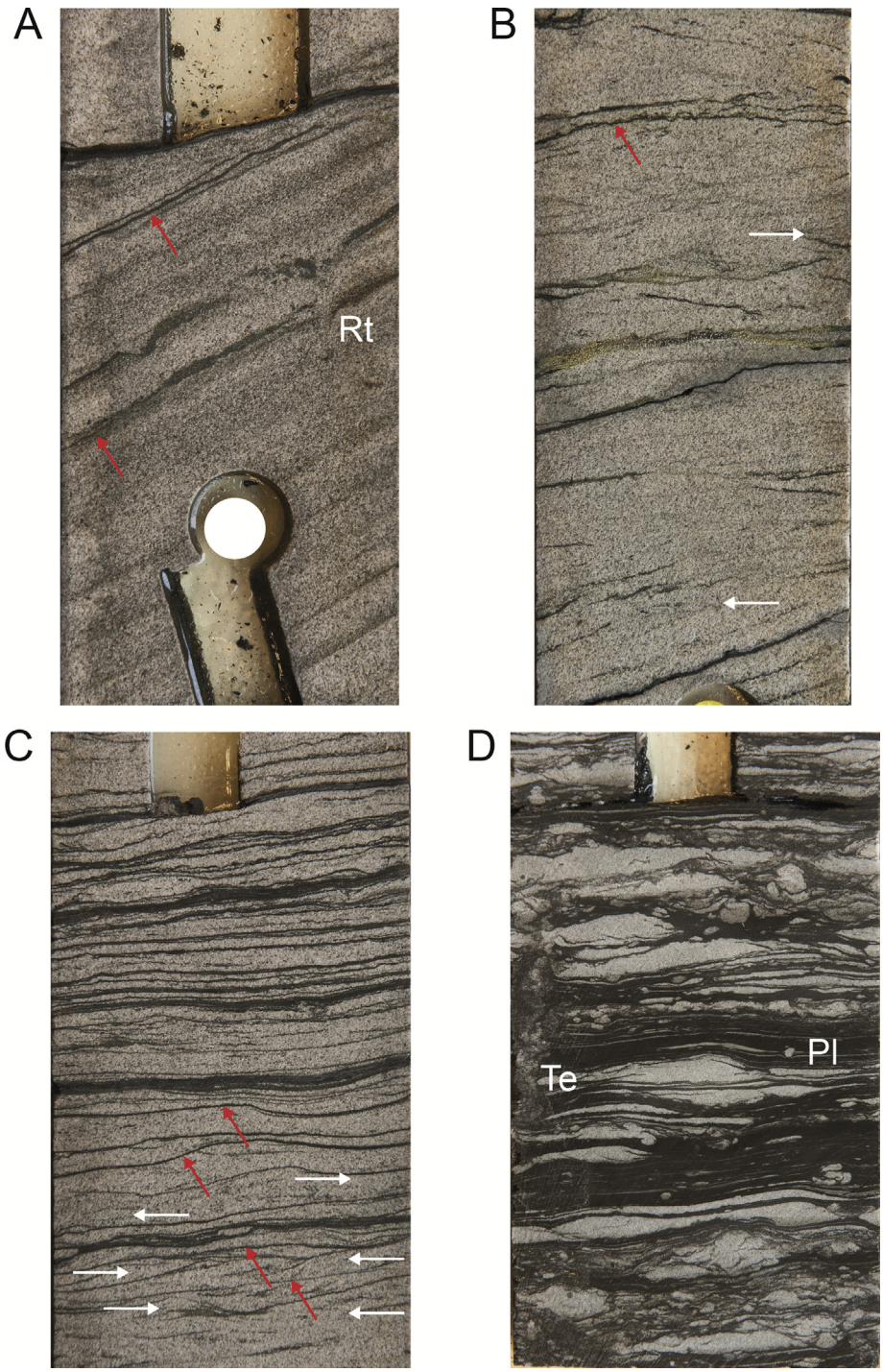

Fig. 19. **A**: Preserved cross-stratified set thicknesses vary between 8 and 15 cm, with well-developed bottomsets in which backflow ripples structures occur (3095.15 m). Double mud drapes and organic particles occur abundantly. **B**: Cross-stratified, well to very well rounded and well-sorted sandstone unit with abundant bidirectional current structures (arrows; 3104.60 m). **C**: Thin sets (up to 10 cm thick) with abundant fluid mud layers (red arrows) and pervasive bidirectionality (white arrows) with an increasing amount of coal fragments (3093.30 m). **D**: Examples of bivalve resting traces (Rt in **A**), *Planolites* (Pl) and *Teichicnus* (Te; 3089.0 m). See also Fig. 15; core width is 9 cm.

Vollset and Doré, 1984; Røe and Steel, 1985; Lervik, 2006) forms the upper part of the Statfjord Group and is encountered across a relatively large part of the Tampen area (Fig. 21). The formation overlies the fluvial Eiriksson Fm and represents the transition from alluvial-deltaic to marine conditions of the Amundsen Fm mudstones with which it is locally contemporaneous (Nystuen and Fält, 1995; Ravnås et al., 2000). The depositional environment envisaged for the Nansen Fm in the Oseberg field is a low-gradient, mixed-energy transgressive delta with wave-dominated shoreline deposits, tidal channels and tidal bars as well as a minor amount of tidal flat and tidal creek deposits (Røe and Steel, 1985; Ryseth, 2001; Statoil in-house data).

In contrast with the thick Tilje Fm example, the two closely spaced almost structureless homogeneous sandstone bed examples in the Nansen Fm are thin (80 cm and 60 cm respectively) and part of an overall fining-upward but heterogeneous sedimentary

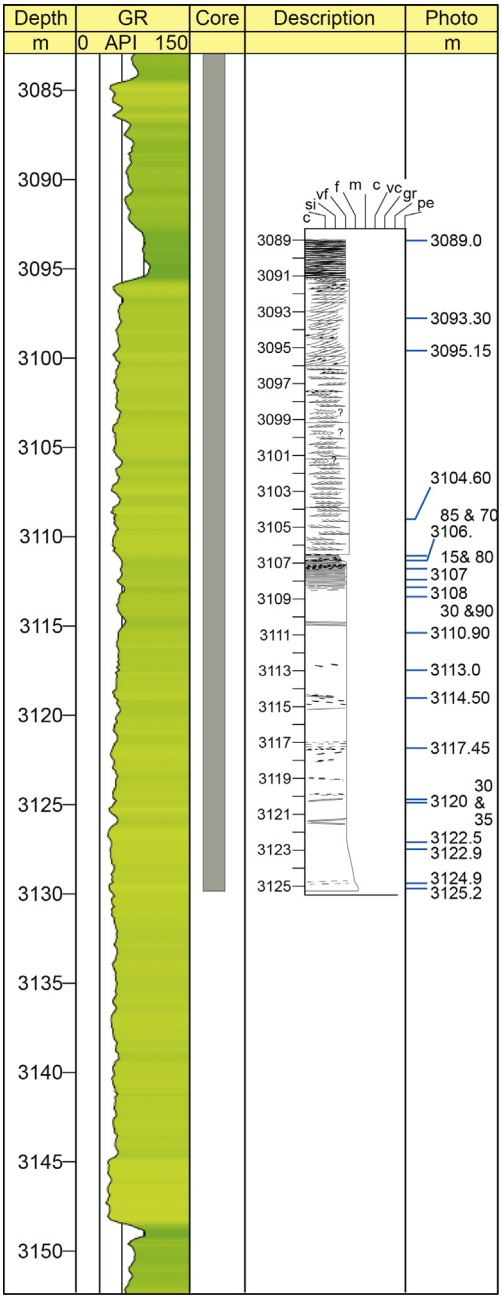

Fig. 20. Gamma-ray (GR) log for the cored part of the well showing a subdivision in two units as indicated by the higher GR readings interpreted to reflect a higher degree of mudstone in the upper unit.

succession of almost 23 m thick (base at 2682.25 m and top at 2659.5 m; Fig. 22B). At the base, this succession is formed by sub-angular, poorly sorted cross-stratified sandstone with abundant coal fragments of up to 1.5 cm long, which erodes into a very fine-grained, well-sorted and ripple-laminated carbonaceous sandstone. Upward, grain sorting improves in association with a decreasing grain size towards lower fine; sedimentary structures are dominated by low-angle or planar lamination. A new erosion event occurs approximately 6 m above the base, overlain by poorly sorted, subrounded, coarse-grained low-angle cross-stratified sandstone. Subsequently, and underlying the first massive sandstone bed, a thinly layered, ripple-laminated (maximum set size of 1.5 cm), organic particle rich and fine-grained sandstone bed occurs with some formsets preserved at the top. This bed is overlain by a homogeneous, in places very faintly laminated but mostly structureless and very fine-grained sandstone bed (80 cm thick; Fig. 22) C1, which is eroded at its top. Two thin, fine-grained and ripple-laminated beds follow and are overlain by the second homogeneous and structureless sandstone bed (60 cm thick; Fig. 22)C2 which has similar characteristics as the first occurrence. Faint lamination occurs at the base of the second bed, and one more erosive event occurs approximately 1.5 m above this second bed. A number of ripple-laminated and lower-medium grained sandstone beds form the final 7 m of the 23 m thick sedimentary succession showing an overall upward fining to very fine-grained, ripple-laminated and well-sorted sandstone.

This 23 m thick heterogeneous sedimentary succession is interpreted as a complex three-stage fill of a relatively small distributary channel in the fluvial to tidal transition zone. The occurrence of an occasional horizontal burrow points to a low degree of salinity influence; possible tidal indicators are rare and indecisive. The two thin but almost structureless homogeneous sandstone beds are interpreted as turbidite deposits that originated from breaching of the margin of the distributary channel and can be classified as non- or slightly erosional sheet-like deposits (SMS) analogous to similar examples in the Vlierzele Sands described above (Fig. 8, situation B or C). Both occurrences are assumed to have been significantly thicker shortly after deposition but to have later been eroded at their top by subsequent scouring events.

6. Other possible breach failure-generated turbidite cases described in the literature

Because the process of breaching is relatively new to the geologists community, so far only the ancient turbidites discussed in this paper have been re-attributed to breach failures, except for one case, the massive sands in the Eocene Brussels Sands (Houthuys, 2011). Other possible examples of breach failure related deposits that show much in common with those of the Vlierzele Sands and the Fell Sandstone are the examples of fluvial deposits reviewed by Martin (1995). These include cases in the Lee-type sandstones (Pennsylvanian) of the central Appalachian Basin, USA, the Mansfield and Brazil Fms (Pennsylvanian) of the Illinois Basin, USA, and the Triassic Hawkesbury Sandstone of the Sydney Basin, Australia. Possibly more candidates will emerge when known examples of massive sands are revisited; this, however, is beyond the scope of this paper. Instead, two cases described in the literature will be discussed shortly, as an illustration of possible breach failure related deposits outside the fluvial and estuarine domain, and in order to stimulate further investigations in the recognition and characteristics of possible breach failure related deposits in other environments. These cases are a tide-influenced marine bay in the vicinity of a spit-barrier complex in the Eocene Brussels Sands, Belgium, and a delta front environment in the Cretaceous of the Bohemian Basin, Czech Republic (Wojewoda, 1986; Uličný, 2001).

The marine, fine to medium grained Brussels Sands example (transition Lower to Middle Eocene) filled, presumably in a relatively short time period, a 40 km wide and over 100 km long tide-influenced marine embayment of the North Sea in Central Belgium (Houthuys, 2011). The process of filling is supposed to have been governed by a barrier-spit complex that protruded into the basin. Because the top of the Brussels Sands has been eroded, the coastal facies of this complex is not preserved. Channels in front of the supposed barrier protrusion were laterally filled in by sand delivered from this coastal complex. Numerous massive to faintly laminated, well sorted sand layers are present, slightly coarser than the surrounding sands, that are inserted in the prevailing west-to-east lateral progradation of the fill (Fig. 23). The panel diagram of

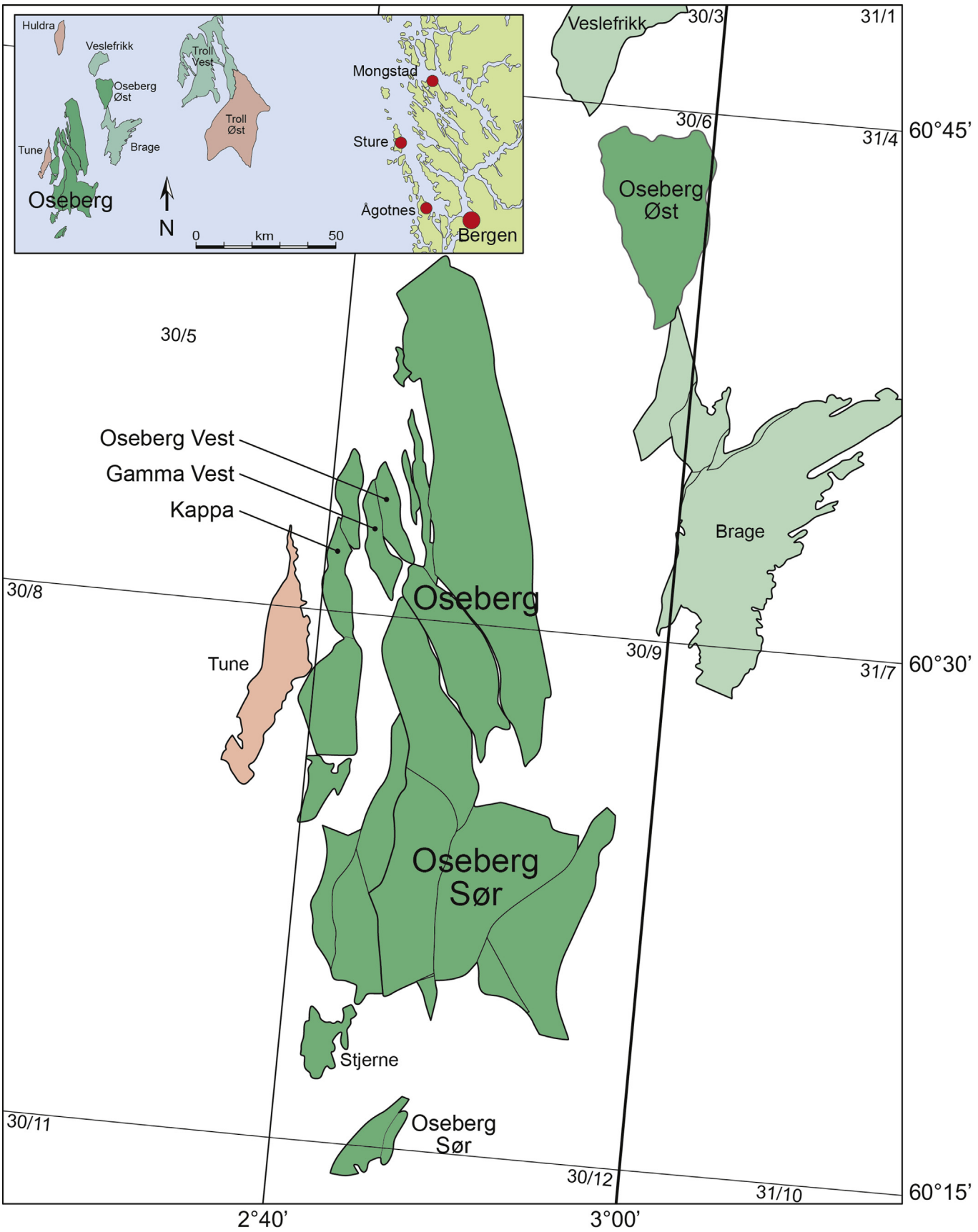

Fig. 21. Location map of the Oseberg West structure (Oseberg field) west-northwest of Bergen.

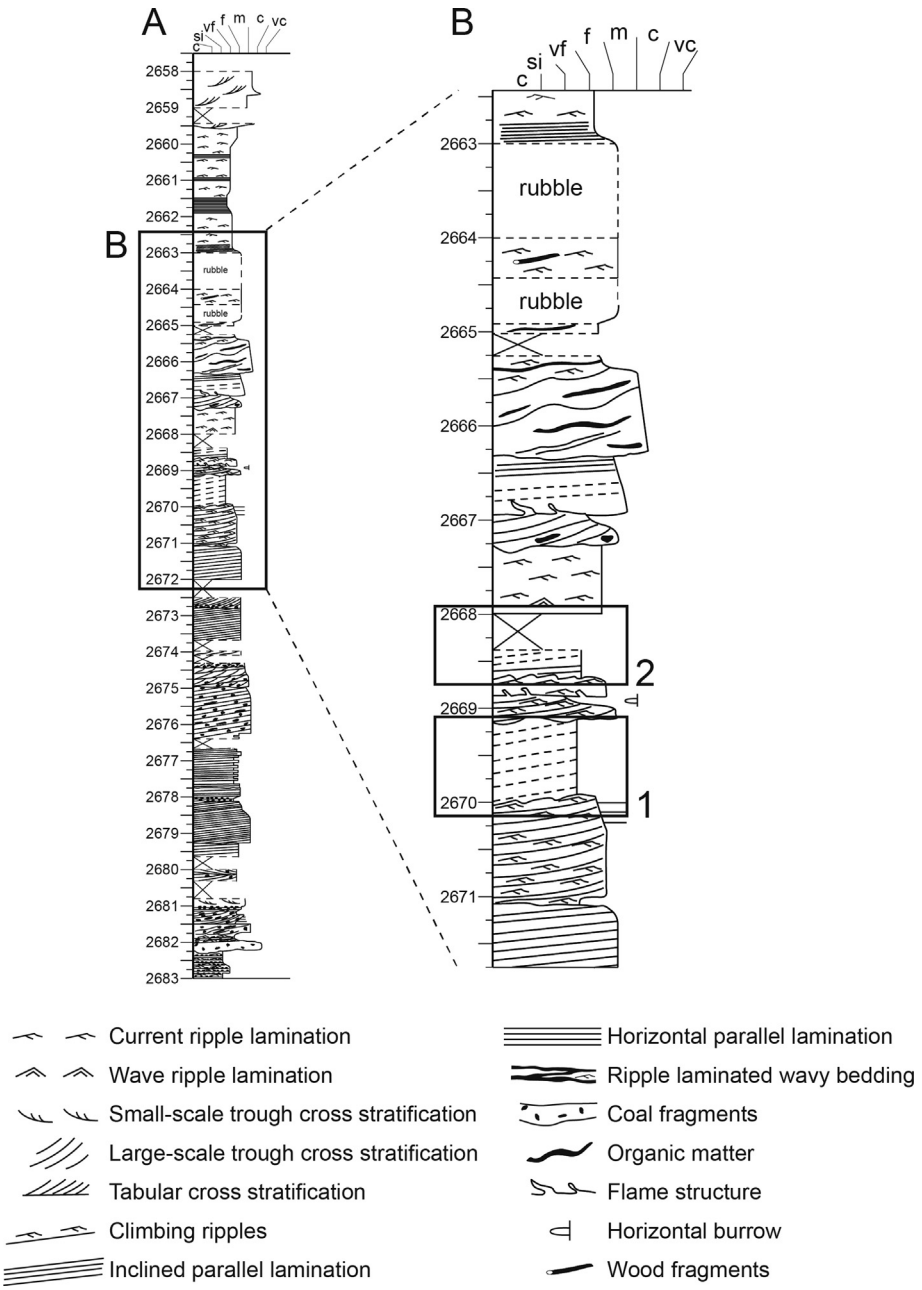

Fig. 22. Core description of the lower part of the Nansen Fm in the Oseberg field showing two relatively thin intervals (1 and 2) interpreted to be formed by breaching; see text for explanation.

Fig. 23 illustrates the sedimentary architecture of the Brussels Sands near Chaumont-Gistoux, situated in the center of the embayment. The mining of a several hectares complex of sandpits at this location was monitored using photography of the sandpit faces from 1986 onwards. Progradation was dominantly from west to east and the succession is formed by alternations of cross-bedded sand (facies X), bioturbated thin cross-beds (Xb), bioturbated beds with the primary thin cross beds still recognizable (Bx), and completely bioturbated, medium sand (Bm). These facies have gradual transitions and all testify to a tidal environment sheltered for waves and storms (Houthuys, 2011). Interpreted successive depositional events producing the massive or faintly laminated facies M are shown in different shades of blue (Fig. 23). Volumes related to the largest individual massive sand bodies (Fig. 23) easily exceed 2 to 5 million m^3. The occurrence of the massive lenses is clearly associated with incisions at the base of the Brussels Sands oriented NNE-SSW, which probably represent channels eroded by tidal currents in front of the eastward expanding barrier-spit complex. Many diagnostic characteristics for breach failure related deposits are found in these lenses: wedge shape of each package; strong, even subvertical incisions, especially near the top of the formation; vertical alternations of faint, sub-horizontal lamination and massive sand bodies (Fig. 24); frequent internal incision features (Figs. 24 and 25); incorporation of intra-formational sand lumps, indicating a relatively short transport distance (Fig. 26) and a complete lack of bioturbation (Fig. 24). The top of the massive sand may show dewatering structures (Fig. 25); so far lower boundaries draping undisturbed bed morphologies

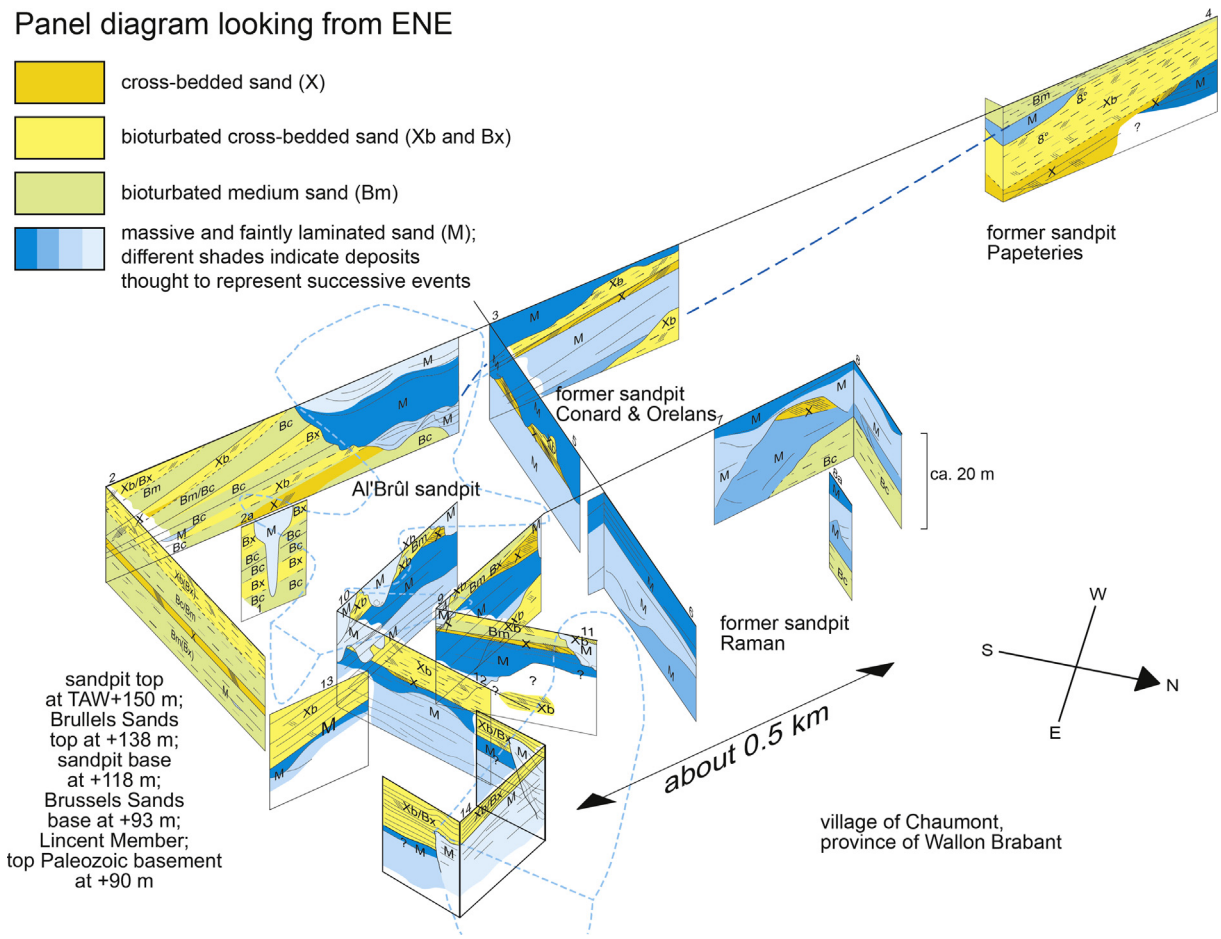

Fig. 23. Panel diagram showing the spatial distribution of facies of the Brussels Sands near Chaumont-Gistoux. For location see Fig. 2. Vertical exaggeration with about a factor 6.

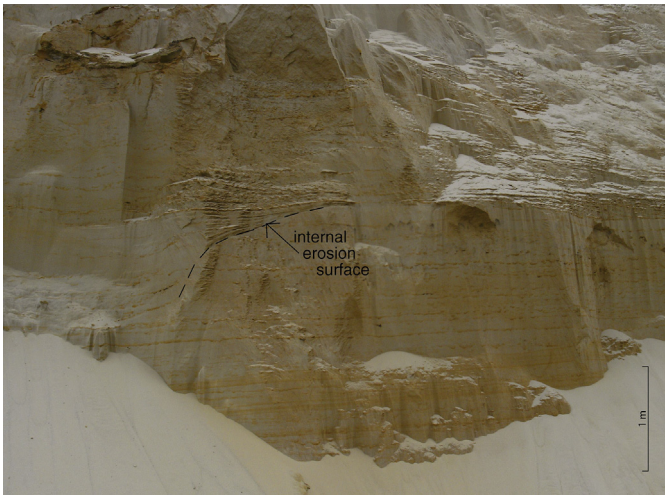

Fig. 24. Brussels Sands. About 1 m deep internal incision (arrow) in a sand deposit with spaced planar lamination curving upwards near the margin of the fill of the incision.

Fig. 25. Brussels Sands: Packages of faint spaced planar lamination in a limonite-cemented section showing evidence of dewatering: wavy deformation of faint laminae (arrows) and dish structures in the upper part of the photo. Length of trowel 40 cm.

have not been found. The ordinary Brussels Sands grading is coarsening upwards. The breaching events provide a mechanism for conveying relatively coarse sand, derived from the upper bank, into the deeper embayment environment.

The second example comes from coarse-grained Gilbert-type deltas in the Middle Turonian to Early Coniacian sandstones of the Bohemian Cretaceous Basin, Czech Republic (Wojewoda, 1986; Uličný, 2001). Gravelly delta foresets packages that pass downslope into a muddy offshore facies contain small incised channels,

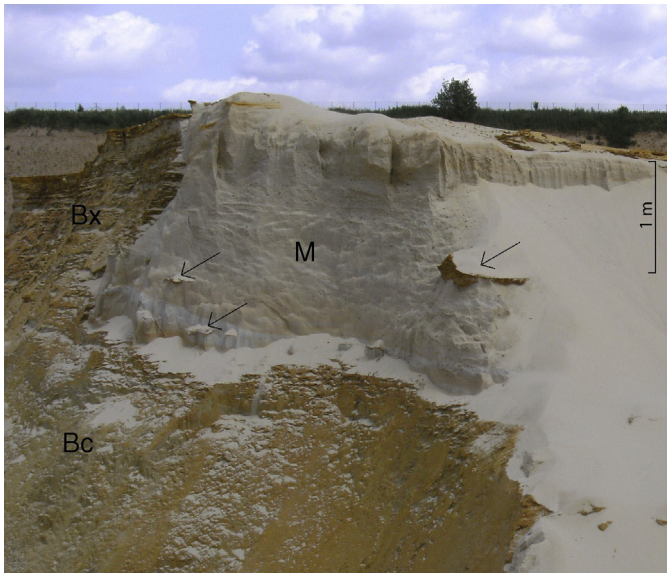

Fig. 26. Brussels Sands. Erosive incision (in bioturbated Bx to strongly bioturbated Bc tidal cross beds) filled with well-sorted, quasi massive sand (labelled M). The massive sand embeds lumps (arrows) eroded of adjacent layers. Note irregular erosive contact showing nearly vertical wall in upper part of the section. Exposed section is approximately 6 m high.

parallel to the foreset slope, filled with fine to medium sand (Fig. 27). Near the foreset toe the channel fills are seemingly structureless to faintly bedded. In the upslope parts of some channel fills, subparallel, slightly undulating laminae occur that pass upslope into backsets. Some of the backsets that, considering their scale, possibly were produced by cyclic steps, pass upwards into spaced planar lamination (Uličný, 2001, Fig. 8d). The channels and their fills were interpreted by Uličný (2001) as being produced by turbidity currents triggered by liquefaction failures in the upper part of the delta foreset slope. However, the long set length of backset bedding could not have been formed in the short spell of such a failure. Two alternative mechanisms could be considered, hyperpycnal flows or breaching. Examples of comparable channel fills interpreted to be generated by hyperpycnal flows suggest that this leads preferentially to fills with relatively coarse sediments (Nielsen et al., 1988; Massari, 1996), which is consistent with the extreme conditions that cause these flows. The sediment of the channel fills in the Bohemian Cretaceous Basin is, however, relatively fine compared to the surrounding foresets. Therefore, a breach failure origin of the channel fills seems more likely. Massive sands are nowhere observed to cover undisturbed pre-existing bed morphologies, which is understandable, as in this case the turbidity current was not blocked by the confinement of a deep but rather narrow channel.

7. Discussion and conclusions

7.1. Breaching conditions

In many situations of steep and long underwater sand slopes, turbidites are considered to be produced by liquefaction failures. In this paper, it is argued, however, that breaching rather than liquefaction is the main failure process. Van den Berg et al. (2002) speculated that breach failures can produce turbidity currents that are able to bring sand to the deep ocean and might explain the origin of thick massive sands found in some ancient deep-water turbidite successions. Numerical computations by Mastbergen and Van den Berg (2003) and Eke et al. (2011) supported the first part of the speculation. These results were based on failure events comprising relatively small volumes of sand, in the order of 0.1–0.2 million m^3. Such volumes are incompatible with the large volumes of sand needed to form turbidite sand lobes with dm - m thick T_{B-4} units on submarine fan lobes. Actually, evidence of historic breach failures (Wilderom, 1979; Torrey, 1995) indicates that breach failure deposits may surpass several million m^3 (Silvis and de Groot, 1995), like measured in the Brussels Sands. Data from among others the Karoo Basin (Prélat et al., 2010), suggest that individual turbidite beds in submarine fan lobes have a sand volume in the order of one to several million m^3. Therefore, a breach failure origin of deep-water massive sands that accumulated quickly in confined basins is likely. To complicate matters, remote from the failure location, turbidity currents produced by both types of failures are sustained and produce the same structureless T_{B-4} unit, without leaving a clue that allows recognition of the type of failure.

A prerequisite condition for the development of large breach failures is the presence of an underwater slope over a considerable depth interval, built or incised in fine to medium sand. According to

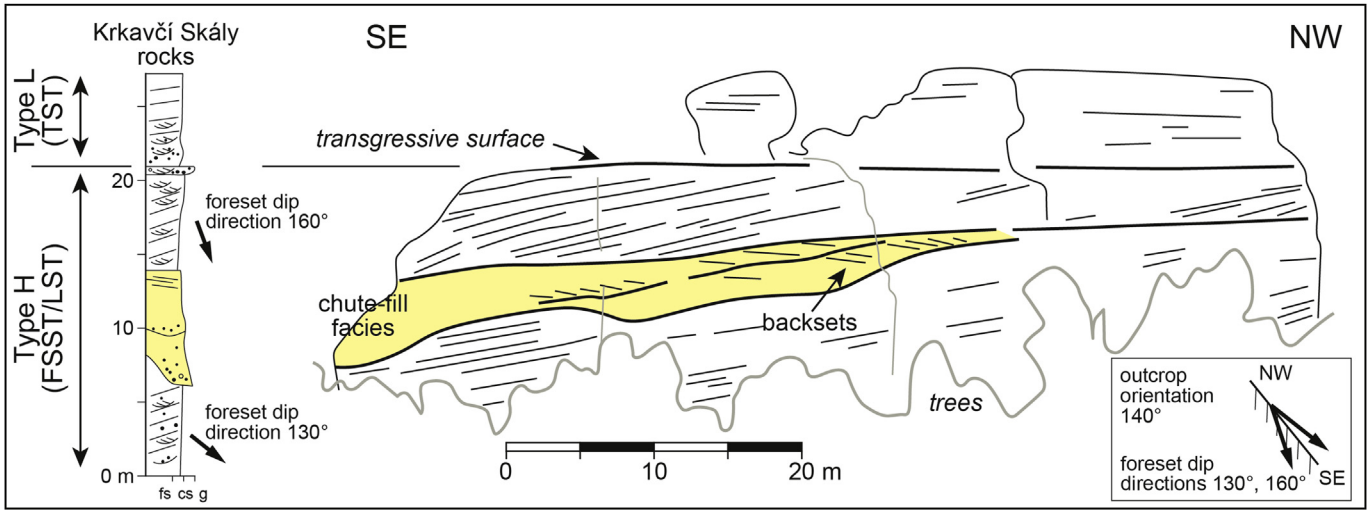

Fig. 27. Deltafront foresets with amalgamated massive-type channel fills in a coarse-grained Gilbert-type delta of the Bohemian Cretaceous Basin (after Uličný, 2001, Fig. 9c).

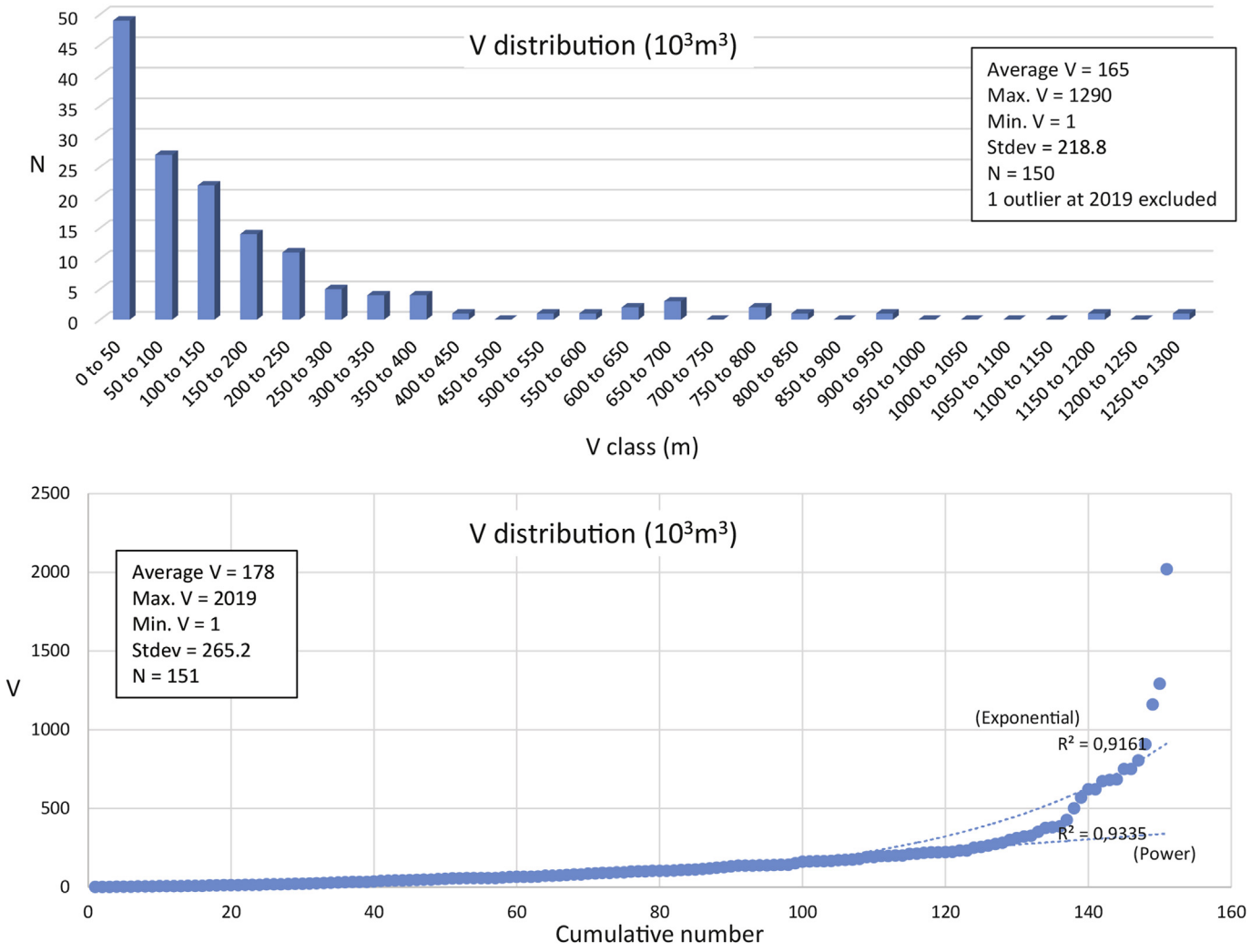

Fig. 28. Descriptive statistics and graphs showing the distribution of breach volume (V) of all observed breaches (N = 150) recorded from the modern Eastern and Western Scheldt as reported in Wilderom (1979).

the data base of bank failures in the SW Netherlands this depth should be at least around 10 m at bankfull stage (Wilderom, 1979; Van den Berg et al., 2002). Therefore, in environments where such slopes in fine sands are common, like channels of large lowland rivers, deep estuarine channels and some nearshore situations, breaching related deposits may be common. This wide variety of environments is supported by the evidence of these deposits from fluvial, estuarine, delta front and shallow marine areas in front of barrier-spit complexes presented in this paper. Breaching related deposits in these environments can be differentiated from deposits of liquefaction failures that also may be found in these areas, because the proximity of the failure implies that the liquefied flow will produce a sandy debrite without any undisturbed primary sedimentary structures. The vertical succession of sedimentary structures in breach failure related deposits that have been deposited close to the failure depends on the hydrography of the area of deposition. In a channel, the turbidity current generated by breaching will be blocked by the opposite channel margin, giving rise to very thick massive sands that may show a non-erosional base. In such cases of channel confinement, apart from these non or hardly erosional sheet-like massive sandbodies (SMS), two other breach failure related architectural elements are formed that may preserve: channel-like massive sands (SMC) and packages of spaced planar lamination (SSL). The recognition of two of these three types of sedimentary structures may be considered proof of a breach failure origin of the deposits.

7.2. Consequences for reservoir characterization

Understanding the distribution, geometry and dimensional properties of lithological heterogeneities in tidally-influenced or -dominated reservoirs at small- (cm to dm) to large-scale (10's of m) is crucial for designing appropriate hydrocarbon drainage strategies. These heterogeneities cause permeability and porosity contrasts and compartmentalization (forming a complex 3D network) that will significantly affect fluid flow patterns. Recovery factors of these heterolithic units are typically below 30% and pose one of the main challenges on the Norwegian continental shelf. To mitigate production risk issues, the characteristics of heterogeneities formed in tidal environments are used to build bedform-scale geomodels of heterolitic tidal units of (for example) the Tilje and Nansen formations. The key to improving predictions of reservoir performance is to represent the observed heterogeneities and associated porosity and permeability properties in 3D from the ripple scale to the bar scale. Working with subsurface reservoirs, geometrical data are typically taken from outcrops and model

realizations are populated with petrophysical data derived from core plug and well log measurements. Upscaling of these petrophysical models subsequently results in effective porosity and permeability values for the tidal facies and is used to generate type curves showing the relationship between permeability and shale volumes. Results indicate how much volume of connected sand must be present before the reservoir will be producible. Consequently, it is important to adequately represent small- and large-scale 3D geometrical data of all facies present in a tidal reservoir and understand their dimensions and formative processes.

Wilderom (1979) presented data on the geometrical aspects of 151 breach failure deposits in the estuaries of The Netherlands that occurred between 1800 and 1978 along estuary banks (two-thirds) as well as on tidal bar flanks (one-third). He noted that the displaced volume of sand during a breach failure on a tidal bar flank is much larger than a breach failure at the estuary bank, mentioning the example of a large tidal bar (the Spijkerplaat, located SE of Flushing, see Fig. 2) were 14.6 million m^3 of fine sand was displaced as the result of 5 breaching events over a period of 11 years. Based on his dataset, Wilderom (1979) noted also that generally one-third of the breached sand volume is transported away within months after the event (depending on the energy distribution in the channel) and two-thirds will remain in place for a longer time period. When considering on the one hand the detailed mapping of a recent breach failure in the Western Scheldt (Fig. 1), and on the other hand the results of a general statistical analysis of 68 breach failures reported in Wilderom (1979; Figs. 28–30), it is obvious that although breach failure related deposits are very common in estuarine environments, can be thick and may contain several million m^3 of fine sand, they are geographically restricted in both transverse and longitudinal section.

The implication of this is that when a thick massive sand layer is encountered in a core (such as the Flyndretind and Oseberg examples), care should be taken to not assign large dimensions to their occurrences in the reservoir characterization and modelling process. When found in a fluvial, tidal or shallow marine setting, these potentially thick and homogeneous, well-sorted sand deposits with good properties for hydrocarbon flow are constricted by the palaeochannel width in which they were deposited and are spatially restricted in length and width. Based on the data of Wilderom (1979; Figs. 28–30), even the thickest and most voluminous breach failure related deposits in tidal channels commonly

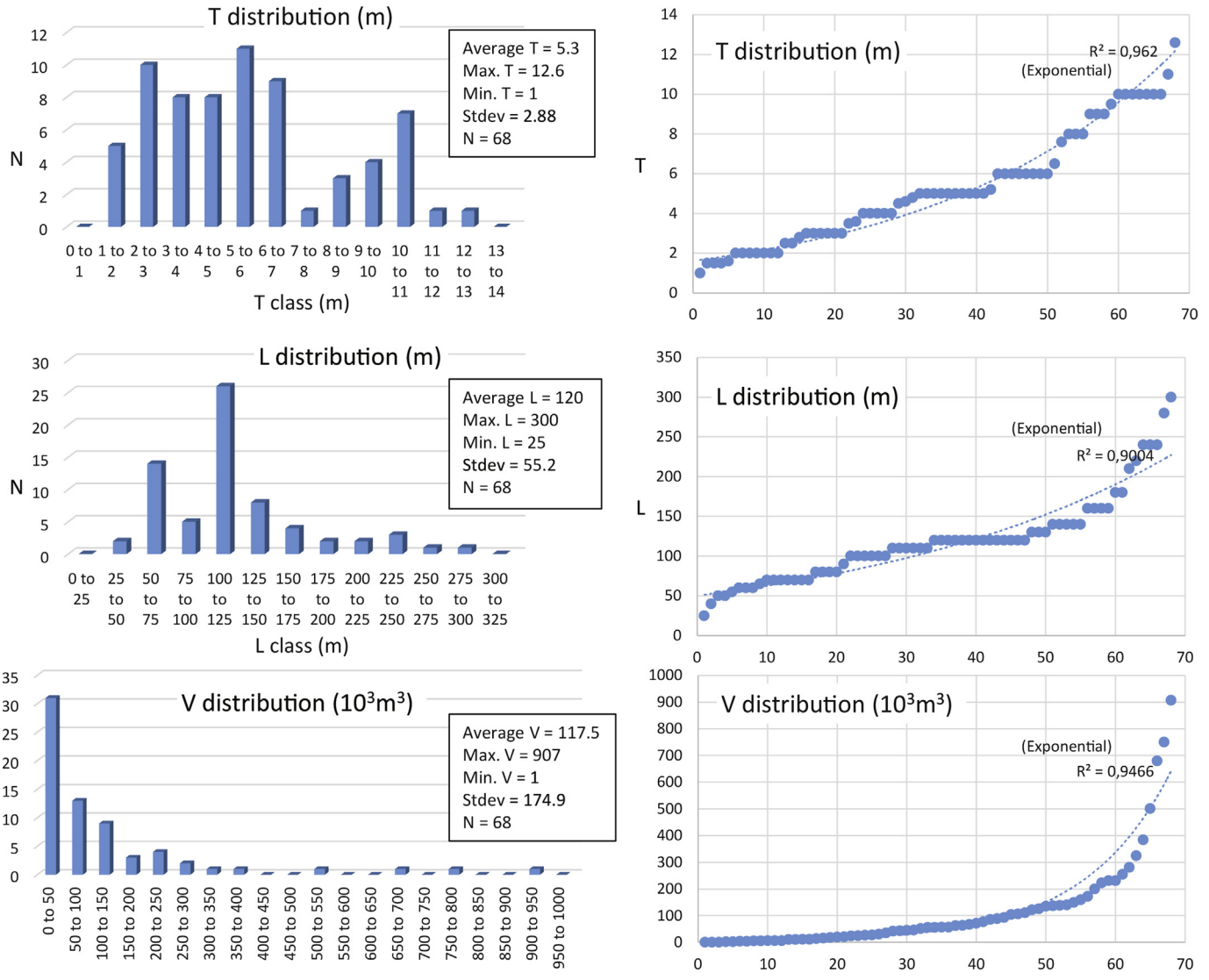

Fig. 29. Descriptive statistics and scatterplots showing the distribution of breach thickness (T), length (L) and volume (V) of breaches that have all 3 parameters recorded (N = 68). Data from the modern Eastern and Western Scheldt as reported in Wilderom (1979).

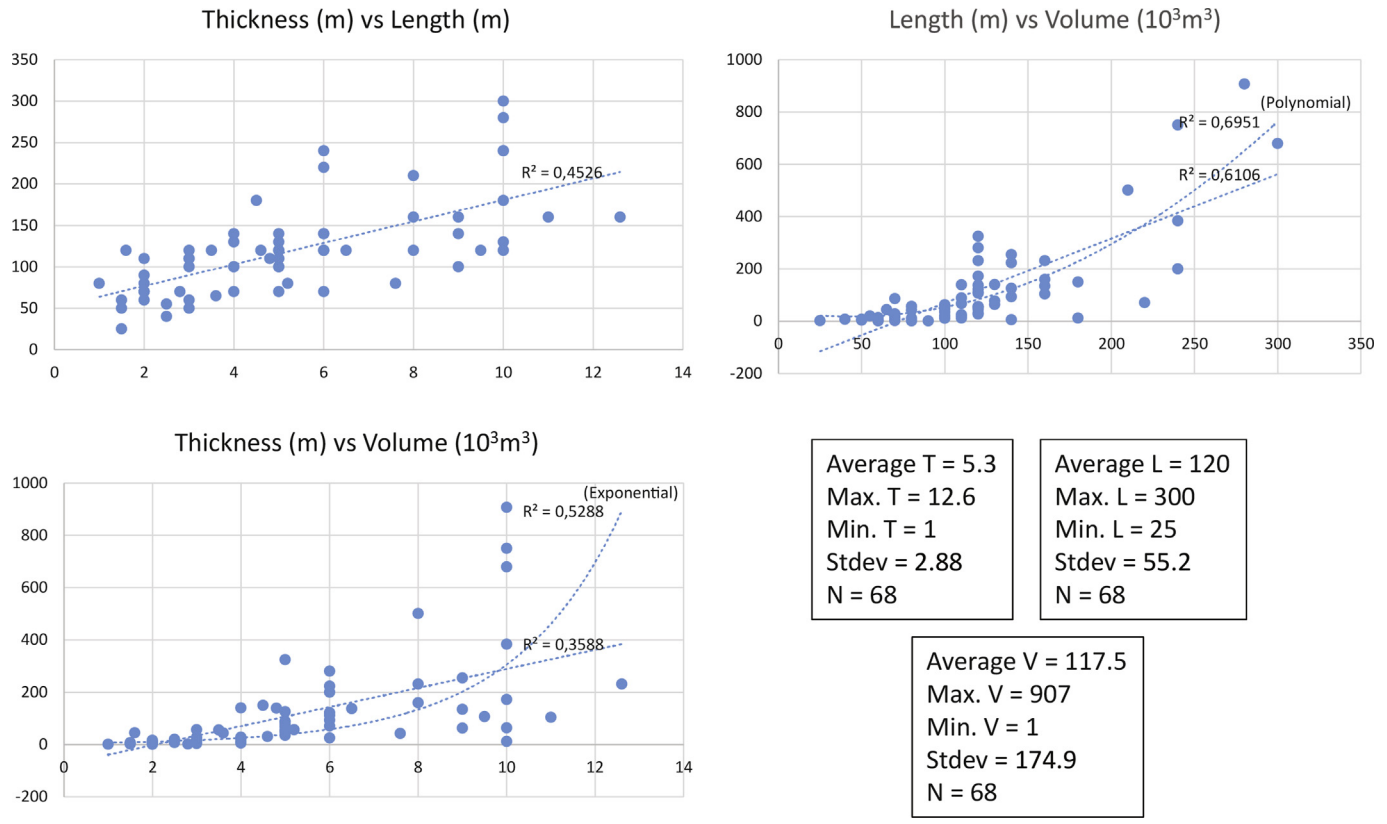

Fig. 30. Descriptive statistics and scatterplots showing the relation between breach thickness versus length, thickness versus volume and length versus volume of breaches that have all 3 parameters recorded (N = 68). Data from the modern Eastern and Western Scheldt as reported in Wilderom (1979). A weak correlation only exists between breach thickness and length.

do not exceed 300 m in transverse (perpendicular to breach failure retrogression) direction. Their longitudinal length is not much more, unless successive breach failures occurred at close distance (Fig. 1A), resulting in an amalgamated massive sand of somewhat larger extension, such as found in the Brussels Sands (Fig. 23). A thick (several meters), homogeneous sandstone occurrence encountered in an oilfield well is often modelled as a laterally continuous unit with good three-dimensional connectivity. However, this is possibly only the case when deposition took place a in deep marine environment. Careful facies interpretation is key to identifying this. When constructing a static reservoir model, the type of environment needs to be considered both for in-place volume calculations as well as for drainage strategy considerations.

Acknowledgements

We thank John Dalrymple of the Northumbrian Mountaineering Club for guiding us to fascinating exposures with massive sands known by climbers of the Bowden Doors and Colour Heugh crags by names such as The Wave, Poseidon, Giants Ear and Turner's Hand, and providing us with splendid photos of the sedimentary structures. We also thank Erik Rasmussen and one anonymous reviewer for comments that improved the manuscript content and structure. Lars Reistad (Statoil ASA) is thanked for his skillful preparation of the illustrations. Statoil ASA is acknowledged for permission to publish the Flyndretind and Oseberg core data.

References

Allen, J.R.L., Collinson, J.D., 1974. The superposition and classification of dunes formed by unidirectional aqueous flows. Sediment. Geol. 12, 169–178.

Beinssen, K., Neil, D.T., Mastbergen, D.R., 2014. Field observations of retrogressive breach failures at two tidal inlets in Queensland, Australia. Aust. Geomech. 49, 55–63.

Beinssen, K., Neil, D.T., 2015. Retrogressive breach failure events at Amity Point, Australia and their interaction with built defences. June 21-26, 2015. In: Proceedings of the Twenty-fifth (2015) International Ocean and Polar Engineering Conference. Kona, Big Island, Hawaii, USA, pp. 1325–1330.

Bouma, A.H., 1962. Sedimentology of Some Flysch Deposits: a Graphic Approach to Facies Interpretation. Elsevier, Amsterdam, p. 168.

Brekke, H., Sjulstad, H.I., Magnus, C., Williams, R.W., 2001. Sedimentary environments offshore Norway – an overview. In: Martinsen, O.J., Dreyer, T. (Eds.), Sedimentary Environments Offshore Norway – Paleozoic to Recent. Norwegian Petroleum Society, Special Publications, 10. Elsevier, Amsterdam, pp. 7–37.

Cartigny, M.J.B., Postma, G., Van Den Berg, J.H., Mastbergen, D.R., 2011. A comparative study of sediment waves and cyclic steps based on geometries, internal structures and numerical modelling. Mar. Geol. 280, 40–56. http://dx.doi.org/10.1016/j.margeo.2010.11.006.

Cartigny, M.J.B., Iacono, L., Urgeles, R., Druet, R.M., Acosta, J., 2017. Cyclic steps in the southern submarine canyons of the Balearic Islands (western Mediterranean). In: Guillén, J., Acosta, J., Chiocci, F.L., Palanques, A. (Eds.), Atlas of Bedforms in the Western Mediterranean. Springer, Switzerland, pp. 223–228. http://dx.doi.org/10.1007/978-3-319-33940-5.

Casalbore, D., Bosman, A., Romagnoli, C., Chiocci, L., 2013. Small-scale crescent-shaped bedforms in submarine volcanic setting: examples from Stromboli island (Italy). GeoActa 12, 301–309.

Casalbore, D., Bosman, A., Ridente, D., Chiocci, F.L., 2014. Coastal and submarine landslides in the tectonically-active Tyrrhenian Calabrian margin (Southern Italy); Examples and geohazard implications. In: Krastel, S., Behrmann, J.-H., Völker, D., Stipp, M., Berndt, C., Urgeles, R., Chaytor, J., Huhn, K., Strasser, M., Harbitz, C.B. (Eds.), Submarine Mass Movements and Their Consequences, Advances in Natural and Technological Hazards Research, vol. 37, pp. 261–269. http://dx.doi.org/10.1007/978-3-319-00972-8 23.

Clare, M.A., Cartigny, M.J.B., North, L.J., Talling, P.J., Vardy, M.E., Hizzett, J.L., Sumner, E.J., Clarke, J.E., Spinewine, B., Cooper, C., 2015. Quantification of near-bed dense layers and implications for seafloor structures: new insights into the most hazardous aspects of turbidity currents. Houston, Texas, USA. In: Proceedings of the Annual Offshore Technology Conference. paper OCT-25705-MS, 12 pp. http://dx.doi.org/10.4043/25705-MS.

Dalland, A., Worsley, D., Ofstad, K., 1988. A lithostratigraphic scheme for the Mesozoic and Cenozoic succession offshore mid- and northern Norway. Nor.

Pet. Dir. Bull. 4, 1–65.
De Batist, M., 1989. Seismostratigrafie en Structuur van het Paleogeen van de Zuidelijke Noordzee. PhD thesis. Universiteit van Gent, p. 107.
De Batist, M., Versteeg, W.H., 1999. Seismic stratigraphy of the Mesozoic and Cenozoic in northern Belgium: main results of a high-resolution reflection seismic survey along rivers and canals. Geol. Mijnb. 77, 17–37. http://dx.doi.org/10.1023/A:1003446611678.
Dilliard, K.A., Simpson, E.L., Noto, R.C., Wizevich, M., 1999. Characterization of fluvial deposits interbedded with flood basalts, neoproterozoic catoctin formation, central appalachians, USA. Precambrian Res. 97, 115–134. http://dx.doi.org/10.1016/S0301-9268(99)00025-X.
Doré, A.G., 1991. The structural foundation and evolution of Mesozoic seaways between Europe and the Arctic. Palaeogeogr. Palaeoclimatol. Palaeoecol. 87, 441–492. http://dx.doi.org/10.1016/0031-0182(91)90144-G.
Eke, E., Viparelli, E., Parker, G., 2011. Field-scale numerical modeling of breaching as a mechanism for generating continuous turbidity currents. Geosphere 7, 1063–1076. http://dx.doi.org/10.1130/GES00607.1.
Gulinck, M., Hacquaert, A., 1954. L'Eocène. In: Fourmarier, P. (Ed.), Prodrome d'une description géologique de la Belgique. Liège Société Géologique de Belgique, pp. 451–493.
Gjelberg, J., Dreyer, T., Høie, A., Tjelland, T., Lilleng, T., 1987. Late Triassic to Mid-Jurassic sandbody development on the Barents and mid-Norwegian shelf. In: Brooks, J., Glennie, K.W. (Eds.), Petroleum Geology of North West Europe, pp. 1105–1129.
Harbitz, C.B., Løvholt, F., Pedersen, G., Masson, D.G., 2006. Mechanisms of tsunami generation by submarine landslides: a short review. Nor. J. Geol. 86, 255–264.
Hiscott, R.N., Middleton, G.V., 1980. Fabric of coarse deep-water sandstones, tourelle formation, Quebec, Canada. J. Sediment. Petrol. 50, 703–722. http://dx.doi.org/10.1306/212F7AC7-2B24-11D7-8648000102C1865D.
Hiscott, R.N., 1994. Traction-carpet stratification in turbidites, fact or fiction. J. Sediment. Petrol. 64, 204–208.
Hjellbakk, A., 1997. Facies and fluvial architecture of a high-energy braided river: the upper proterozoic seglodden member, varanger peninsula, northern Norway. Sediment. Geol. 114, 131–161. http://dx.doi.org/10.1016/S0037-0738(97)00075-4.
Houthuys, R., 1990. Vergelijkende Studie van de Afzettingen van Getijdezanden uit het Eoceen en van de huidige Vlaamse Banken. PhD thesis. In: Aardkundige Mededelingen, vol. 5. Universiteit van Leuven, p. 137.
Houthuys, R., Gullentops, F., 1988. The Vlierzele Sands (Eocene, Belgium): a tidal ridge system. In: De Boer, P.L., Van Gelder, A., Nio, S.D. (Eds.), Tide-influenced Sedimentary Environments and Facies. Reidel, Dordrecht, pp. 139–152.
Houthuys, R., 2011. A sedimentary model of the Brussels sands, Eocene, Belgium. Geol. Belg. 14, 55–74.
Hughes Clarke, J.E., 2016. First wide-angle view of channelized turbidity currents links migrating cyclic steps to flow characteristics. Nat. Commun. 7, 1–13. http://dx.doi.org/10.1038/ncomms11896.
Ichaso, A.A., Dalrymple, R.W., 2014. Eustatic, tectonic and climatic controls on an early syn-rift mixed-energy delta, Tilje Formation (Early Jurassic, Smørbukk field, offshore mid-Norway). IAS Special Publication 46. In: Martinius, A.W., Ravnås, R., Howell, J.A., Steel, R.J., Wonham, J. (Eds.), From Depositional Systems to Sedimentary Successions on the Norwegian Continental Margin, pp. 339–388. http://dx.doi.org/10.1002/9781118920435.ch13.
Ichaso, A.A., Dalrymple, R.W., Martinius, A.W., 2016. Basin analysis and sequence stratigraphy of the syn-rift Tilje Formation (Early Jurassic), Halten Terrace giant oil and gas fields, offshore mid-Norway. Am. Assoc. Pet. Geol. Bull. 100, 1329–1375. http://dx.doi.org/10.1306/02251614081.
Jones, B.G., Rust, B.R., 1983. Massive sandstone facies in the Hawkesbury Sandstone, a Triassic fluvial deposit near Sydney, Australia. J. Sediment. Petrol. 53, 1249–1259. http://dx.doi.org/10.1306/212F8355-2B24-11D7-8648000102C1865D.
Keogh, K.J., Leary, S., Martinius, A.W., Scott, A.S.J., Riordan, S., Gowland, S., Taylor, A.M., 2014. Data capture for multi-scale modelling of the lourinhã formation, lusitanian basin, Portugal: an outcrop analogue for the Statfjord Group, norwegian North Sea. Special Publications 387. In: Martinius, A.W., Howell, J.A., Good, T.R. (Eds.), Sediment Body Geometry and Heterogeneity: Analogue Studies for Modelling the Subsurface. Geological Society of London, pp. 27–56. http://dx.doi.org/10.1144/SP387.11.
Kneller, B.C., Branney, J., 1995. Sustained high-density turbidity currents and the deposition of thick massive sands. Sedimentology 42, 607–616.
Lervik, K.-S., 2006. Triassic lithostratigraphy of the northern North Sea basin. Nor. J. Geol. 86, 93–116.
Lowe, D.R., 1982. Sedimentary gravity flows: II. Depositional models with special reference to the deposits of high density turbidity currents. J. Sediment. Petrol. 52, 279–297.
Macías, J.L., Capra, L., Scott, K.M., Espindola, J.M., García-Palomo, A., Costa, J.E., 2004. The 26 May 1982 breakout flows derived from failure of a volcanic dam at El Chichón, Chiapas, Mexico. Geol. Soc. Am. Bull. 116, 233–246. http://dx.doi.org/10.1130/B25318.1.
Malgesini, G., Talling, P.J., Hogg, A.J., Armitage, D., Goater, A., Felletti, F., 2015. Quantitative analysis of submarine-flow deposit shape in the Marnoso-Arenacea formation: what is the signature of hindered settling from dense near-bed layers? J. Sediment. Res. 85, 170–191. http://dx.doi.org/10.2110/jsr.2015.15.
Martin, C.A.L., 1995. The Origins of Massive Sandstones in Braided River Systems. Unpublished PhD Thesis. University of Durham, UK, p. 372.
Martin, C.A.L., Turner, B.R., 1998. Origins of massive-type sandstones in braided river systems. Earth Sci. Rev. 44, 15–38. http://dx.doi.org/10.1016/S0012-8252(98)00019-1.
Martinius, A.W., Kaas, I., Næss, A., Helgesen, G., Kjærefjord, J.M., Leith, D.A., 2001. Sedimentology of the heterolithic and tide-dominated Tilje formation (early jurassic, halten Terrace, offshore mid-Norway). Special Publications, 10. In: Martinsen, O.J., Dreyer, T. (Eds.), Sedimentary Environments Offshore Norway – Paleozoic to Recent. Norwegian Petroleum Society. Elsevier, Amsterdam, pp. 103–144. http://dx.doi.org/10.1016/S0928-8937(01)80011-4.
Martinius, A.W., Van den Berg, J.H., 2011. Atlas of Sedimentary Structures in Estuarine and Tidally-influenced River Deposits of the Rhine-meuse-scheldt System: Their Application to the Interpretation of Analogous Outcrop and Subsurface Depositional Systems. EAGE publications, Houten, p. 298.
Massari, F., 1996. Upper Flow-regime stratification types on steep-face, coarse-grained, Gilbert-type progradational wedges (Pleistocene, southern Italy). J. Sediment. Res. 66, 364–375.
Mastbergen, D.R., Van den Berg, J.H., 2003. Breaching in fine sands and the generation of sustained turbidity currents in submarine canyons. Sedimentology 50, 625–637. http://dx.doi.org/10.1046/j.1365-3091.2003.00554.x.
Mastbergen, D.R., Van den Ham, G.A., Cartigny, M.J.B., Koelewijn, A., de Kleine, M., Clare, M., Hizzett, J., Azpiroz, M., Vellinga, A., 2016. Multiple flow slide experiment in the Westerschelde Estuary, The Netherlands. In: Lamarche, G., Mountjoy, J., Bull, S., Hubble, T., Krastel, S., Lane, E., Micallef, A., Moscardelli, L., Mueller, C., Pecher, I., Woelz, S. (Eds.), Submarine Mass Movements and Their Consequences, Advances in Natural and Technological Hazards Research, vol. 41, pp. 241–252. http://dx.doi.org/10.1007/978-3-319-20979-1_24.
Mazières, A., Gillet, H., Castelle, B., Mulder, T., Guyot, C., Garlan, T., Mallet, C., 2014. High-resolution morphobathymetric analysis and evolution of Capbreton submarine canyon head (Southeast Bay of Biscay—french Atlantic Coast) over the last decade using descriptive and numerical modeling. Mar. Geol. 351, 1–12. http://dx.doi.org/10.1016/j.margeo.2014.03.001.
Meijer, K.L., Van Os, A.G., 1976. Pore pressures near moving underwater slope. Journal of the Geotechnical Engineering Division. Am. Soc. Civ. Eng. 102, 361–372.
Monro, M., 1986. Sedimentology of the Carboniferous Fell Sandstone Group of Northumberland. PhD Thesis. University of Newcastle-upon-Tyne, UK, p. 386.
Mostaert, F., 1985. Bijdrage tot de Kennis van de Kwartairgeologie van de Oostelijke Kustvlakte op Basis van Sedimentologisch en Lithostratigrafisch Onderzoek. PhD Thesis. Universiteit van Gent, p. 587.
Nedelec, Y., Revel, J., 2015. Phénomènes d'érosion côtière: instabilité et consolidation de talus littoraux sur la facade est du cap Ferret (Gironde). May 2015. Rencontres Universitaires de Génie Civil, Bayonne, France.
Nielsen, L.H., Johannessen, P.N., Surlyk, F., 1988. A Late Pleistocene coarse-grained spit-platform sequence in northern Jylland, Denmark. Sedimentology 35, 915–937.
Nordahl, K., Ringrose, P.S., 2008. Identifying the representative elementary volume for permeability in heterolithic deposits using numerical rock models. Math. Geosci. 40, 753–771. http://dx.doi.org/10.1007/s11004-008-9182-4.
Nordahl, K., Messina, C., Berland, H., Rustad, A.B., Rimstad, E., 2014. Impact of multiscale modelling on predicted porosity and permeability distributions in the fluvial deposits of the upper lunde member (snorre field, norwegian continental shelf). Special Publication. In: Martinius, A.W., Howell, J.A., Good, T.R. (Eds.), Sediment-body Geometry and Heterogeneity: Analogue Studies for Modelling the Subsurface, vol. 387. Geological Society of London, pp. 85–109. http://dx.doi.org/10.1144/SP387.10.
Nystuen, J., Fält, L.-M., 1995. Special Publications. In: Hanslien, S. (Ed.), Upper Triassic-lower Jurassic Reservoir Rocks in the Tampen Spur Area, Norwegian North Sea, vol. 4. Norwegian Petroleum Society, pp. 135–179.
Parker, G., 1996. Some speculations on the relation between channel morphology and channel-scale flow structures. In: Ashworth, P.J., Bennett, S.J., Best, J.L., McLelland, S. (Eds.), Coherent Flow Structures in Open Channels. Wiley, Chichester, U.K, pp. 423–458. http://dx.doi.org/10.1016/S0928-8937(06)80041-X.
Paull, C.K., Caress, D.W., Lundsten, L., Gwiazda, R., Anderson, K., McGann, Conrad, J., Edwards, B., Sumner, E.J., 2013. Anatomy of the La jolla submarine canyon system; offshore southern California. Mar. Geol. 335, 16–34.
Postma, G., Cartigny, M.J.B., 2014. Supercritical turbidity currents and their origin, a synthesis. Geology 42, 987–990. http://dx.doi.org/10.1130/G35957.
Postma, G., Cartigny, M.J.B., Kleverlaan, K., 2009. Structureless, coarse-tail graded Bouma Ta formed by internal hydrualic jump of the turbidity current? Sediment. Geol. 219, 1–6. http://dx.doi.org/10.1016/j.sedgeo.2009.05.018.
Postma, G., Kleverlaan, K., Cartigny, M.J.B., 2014. Recognition of cyclic steps in sandy and gravelly turbidite sequences, and consequences for the Bouma facies model. Sedimentology 61, 2268–2290. http://dx.doi.org/10.111/sed.12135.
Prélat, A., Covault, J.A., Hodgson, D.M., Fildani, A., Flint, S.S., 2010. Intrinsic controls on the range of volumes, morphologies, and dimensions of submarine lobes. Sediment. Geol. 232, 66–76. http://dx.doi.org/10.1016/j.sedgeo.2010.09.010.
Ravnås, R., Nøttvedt, A., Steel, R., Windelstad, J., 2000. Syn-rift sedimentary architectures in the northern North Sea. Geological society. Geol. Soc. Spec. Publ. 167, 133–177. http://dx.doi.org/10.1144/GSL.SP.2000.167.01.07.
Reesink, A.J.H., Bridge, J.S., 2011. Evidence of bedform superimposition and flow unsteadiness in unit-bar deposits, South Saskatchewan River, Canada. J. Sediment. Res. 81, 814–840. http://dx.doi.org/10.2110/jsr.2011.69.
Ringrose, P.S., Martinius, A.W., Alvestad, J., 2008. Multiscale geological reservoir modelling in practice. Special Publications. In: Robinson, A., Griffiths, P., Price, S., Hegre, J., Muggeridge, A. (Eds.), The Future of Geological Modelling in

Hydrocarbon Development, vol. 309. Geological Society, London, pp. 123–134. http://dx.doi.org/10.1144/SP309.9.
Rust, B.R., Jones, B.G., 1987. The Hawkesbury Sandstone south of Sydney, Australia: Triassic analogue for the deposit of a large, braided river. J. Sediment. Petrol. 57, 222–233. http://dx.doi.org/10.1306/212F8AEE-2B24-11D7-8648000102C1865D.
Røe, S.-L., Steel, R., 1985. Sedimentation, seal-level rise and tectonics at the triassic-jurassic boundary (Statfjord formation), tampen spur, northern North Sea. J. Pet. Geol. 8, 163–186.
Ryseth, A., 2001. Sedimentology and palaeogeography of the Statfjord Fm (Rhaetian-Sinemurian), North Sea. In: Martinsen, O.J., Dreyer, T. (Eds.), Sedimentary Environments Offshore Norway - Paleozoic to Recent. Elsevier Science, pp. 67–85. http://dx.doi.org/10.1016/S0928-8937(01)80009-6.
Silvis, F., de Groot, M.B., 1995. Flow slides in The Netherlands: experience and engineering practice. Can. Geotechnical J. 32, 1086–1092.
Smith, D.P., Ruiz, G., Kvitek, R., Iampietro, P.J., 2005. Semi-annual patterns of erosion and deposition in Upper Monterey Canyon from serial multibeam bathymetry. Geol. Soc. Am. Bull. 117, 1123–1133. http://dx.doi.org/10.1130/B25510.1.
Smith, D.P., Kvitek, R., Ruiz, G., Iampietro, P.J., Wong, K., 2007. Twenty-nine months of geomorphic change in upper Monterey Canyon (2002–2005). Mar. Geol. 236, 79–94. http://dx.doi.org/10.1016/j.margeo.2006.09.024.
Steurbaut, E., De Ceukelaire, M., Lanckacker, T., Matthijs, J., Stassen, P., Van Baelen, H., Vandenberghe, N., 2016. Lithostratigraphy Ieper Group. Text available on. National Commission for Stratigraphy Belgium. http://ncs.naturalsciences.be/Paleogene-Neogene/proposals-and-discussions.
Stow, D.A.V., Johansson, M., 2000. Deep-water massive sands: nature, origin and hydrocarbon implications. Mar. Pet. Geol. 17, 145–174. http://dx.doi.org/10.1016/S0264-8172(99)00051-3.
Sumner, E.J., Lawrence A. Amy, L.A., Talling, P.J., 2008. Deposit structure and processes of sand deposition from decelerating sediment suspensions. J. Sediment. Res. 78, 529–547.
Sumner, E.J., Talling, P.J., Amy, L.A., Wynn, R.B., Stevenson, C.J., Frenz, M., 2012. Facies architecture of individual basin-plain turbidites: comparison with existing models and implications for flow processes. Sedimentology 59, 1850–1887. http://dx.doi.org/10.1111/j.1365-3091.2012.01329.x.
Talling, P.J., Masson, D.G., Sumner, E.J., Malgesini, G., 2012. Subaqueous sediment density flows: depositional processes and deposit types. Sedimentology 59, 1937–2003. http://dx.doi.org/10.1111/j.13653091.2012.01353.
Torrey, V.H., 1995. Flow slides in Mississippi riverbanks. In: Thorne, C.R., Abt, S.R., Barendt, B.J., Maynard, S.T., Pilarczyk, K.W. (Eds.), River, Coastal and Shoreline Protection- Erosion Control Using Riprap and Armourstone. Wiley, Chichester, pp. 361–377.
Turner, B.R., Monro, M., 1987. Channel formation and migration by mass-flow processes in the lower carboniferous fluviatile Fell sandstone Group, north-east England. Sedimentology 34, 1107–1122.
Uličný, D., 2001. Depositional systems and sequence stratigraphy of coarse-grained deltas in a shallow-marine, strike-slip setting: the Bohemian Cretaceous Basin, Czech Republic. Sedimentology 48, 599–628. http://dx.doi.org/10.1046/j.1365-3091.2001.00381.
Van de Weerd, A.A., 1996. Reservoir geology of the shallow-marine early jurassic Tilje formation of the njord field, offshore Mid-Norway (Final Report European Community, Joule Program, I). In: Johnson, H.D., Wonham, J.P., Gupta, R. (Eds.), Geological Characterisation of Shallow Marine Sands for Reservoir Modelling and High Resolution Stratigraphic Analysis.
Van den Berg, J.H., Van Gelder, A., Houthuys, R., 1998. Possible occurrence of deposits of flow slides in the Eocene Vlierzele Sand, Belgium, a preliminary note. In: Kroon, A., Ruessink, R. (Eds.), Geographical Developments in Coastal Morphodynamics, a Tribute to Joost Terwindt. Faculteit Ruimtelijke Wetenschappen, Utrecht University, Netherlands, pp. 27–43.
Van den Berg, J.H., Van Gelder, A., Mastbergen, D.R., 2002. The importance of breaching as a mechanism of subaqueous slope failure in fine sand. Sedimentology 49, 81–95. http://dx.doi.org/10.1111/j.1525-139X.2006.00168.x-i1.
Van Duinen, A., Bezuijen, A., Van den Ham, G.A., Hopman, V., 2013. Field Measurements to investigate submerged slope failures. In: Krastel, S., Behrmann, J.-H., Völker, D., Stipp, M., Berndt, C., Urgeles, R., Chaytor, J., Huhn, K., Strasser, M., Harbitz, C.B. (Eds.), Submarine Mass Movements and Their Consequences, Advances in Natural and Technological Hazards Research, vol. 37, pp. 13–21. http://dx.doi.org/10.1007/978-3-319-00972-8 2.
Van Rhee, C., Bezuijen, A., 1998. The breaching of sand investigated in large-scale model tests. Proceedings of the International Coastal Engineering Conference. Cph. Am. Soc. Civ. Eng. 3, 2509–2519. http://dx.doi.org/10.1061/9780784404119.189.
Vollset, J., Doré, A., 1984. A revised triassic and jurassic lithostratigraphic nomenclature for the norwegian North Sea. Nor. Pet. Dir. Bull. 3, 1–53.
Wilderom, M.H., 1979. Resultaten van het vooroeveronderzoek langs de Zeeuwse Stromen. Report 75.2. Rijkswaterstaat, Vlissingen, The Netherlands.
Wojewoda, J., 1986. Fault-scarp induced shelf sand bodies: Turonian of the Intrasudetic Basin. In: Teisseyre, A.K. (Ed.), IAS 7th European Regional Meeting Excursion Guidebook. Ossolineum, Wroclaw, Poland, pp. 31–52.
You, Y., Flemings, P., Mohrig, D., 2014. Mechanics of dual-mode dilative failure in subaqueous sediment deposits. Earth Planet. Sci. Lett. 397, 10–18. http://dx.doi.org/10.1016/j.epsl.2014.04.024.